Differential and Numerically Invariant
Signature Curves Applied to Object Recognition

Eugenio Calabi[†]
Department of Mathematics
University of Pennsylvania
Philadelphia, PA   19066-1102
calabi@math.upenn.edu

Peter J. Olver[‡]
School of Mathematics
University of Minnesota
Minneapolis, MN   55455
olver@ima.umn.edu

Chehrzad Shakiban
Department of Mathematics
University of St. Thomas
St. Paul, MN   55105-1096
c9shakiban@stthomas.edu

Allen Tannenbaum[§]
Department of Electrical Engineering
University of Minnesota
Minneapolis, MN   55455
tannenba@ee.umn.edu

Steven Haker
School of Mathematics
University of Minnesota
Minneapolis, MN   55455
haker@math.umn.edu

May 1, 1996

Abstract. In this paper we introduce a new paradigm, the differential invariant signature curve or manifold, for the invariant recognition of visual objects. A general theorem of É. Cartan implies that two curves are related by a group transformation if and only if their signature curves are *identical*. The important examples of the Euclidean and equi-affine groups are discussed in detail. Secondly, we show how a new approach to the numerical approximation of differential invariants, based on suitable combination of joint invariants of the underlying group action, allows one to numerically compute differential invariant signatures in a fully group-invariant manner. Applications to a variety of fundamental issues in vision, including detection of symmetries, visual tracking, and reconstruction of occlusions, are discussed.

2

1. Introduction.

Lie group methods have proven to play a vital role in modern research in computer vision and engineering. Indeed, certain visually-based symmetry groups and their associated differential invariants have, in recent years, assumed great significance in practical image processing and object recognition. Recent surveys can be found in the papers appearing in earlier volumes [**36**], [**37**], [**45**], and, in particular, the review papers [**40**], [**53**]. For reasons of space, we shall not attempt to survey the multitudinous applications of differential invariants to object recognition and geometric diffusion-based multi-scale smoothing, referring the interested reader to the preceding references.

Our approach to differential invariants in computer vision is governed by the following philosophy. We begin with a finite-dimensional transformation group G acting on a space E, representing the image space, whose subsets are the objects of interest. In visual applications, the group G is typically either the Euclidean, affine, similarity, or projective group. We are particularly interested in how the geometry, in the sense of Klein, induced by the transformation group G applies to (smooth) submanifolds contained in the space E. A differential invariant I of G is a real-valued function, depending on the submanifold and its derivatives at a point, which is unaffected by the action of G. In general, a transformation group admits a finite number of fundamental differential invariants, $I_1, \ldots, I_N$, and a system of invariant differential operators $\mathcal{D}_1, \ldots, \mathcal{D}_n$, equal in number to the dimension of the submanifold, and such that every other differential invariant is a function of the fundamental differential invariants and their successive derivatives with respect to the invariant differential operators. This result dates back to the original work of S. Lie, [**32**]; see [**38**] for further historical remarks and a modern exposition. For example, in the Euclidean geometry of curves in the plane, the group action is provided by the Euclidean group consisting of translations and rotations, and every differential invariant is a function of the Euclidean curvature and its derivatives with respect to Euclidean arc length. Similarly, for affine planar geometry, the underlying group is the equi-affine group of area-preserving affine transformations, and every differential invariant of a curve is a function of the affine curvature and its various derivatives with respect to affine arc length.

The fact that, for transitive group actions, an object can be fully reconstructed, modulo group transformations, from a prescribed (and finite) collection of differential invariants, is a consequence of a powerful general theorem due to É. Cartan, [**11**], [**25**]. For example, a curve in the Euclidean plane is uniquely determined, modulo translation and rotation, from its curvature invariant κ and its first derivative with respect to arc length κ_s. Thus, the curve is uniquely prescribed by its *Euclidean signature curve*, parametrized by the two functions (κ, κ_s). Similarly, a curve in the affine plane is uniquely determined, modulo an affine transformation, by its *affine signature curve* which is the planar curve parametrized by the affine curvature and its derivative with respect to affine arc length. This definition of signature offers significant advantages over the traditional approach, [**7**], [**18**], [**44**], [**48**], which is based on the analysis of curvature as a function of arc length, in that a) it avoids an ambiguity in the choice of initial point on the curve, b) it obviates the computational difficulty of reparametrizing the curve in terms of its arc length, and c) it readily extends, via Cartan's general theorem, to surfaces and higher-dimensional submanifolds. A variety of signature curves, both Euclidean and affine, can be found in

the figures at the end of this paper.

In practical applications of invariant theory to computer vision, one is forced to compute a differential invariant, such as the curvature of a curve, by a discrete numerical approximation. A robust and efficient numerical implementation is crucial, but is a nontrivial problem in that the more important differential invariants depend on high order derivatives and are thus particularly sensitive to noise and round-off error. Although the differential invariants reflect the invariance of the image under a transformation group, most standard numerical approximation schemes fail to incorporate this symmetry. Consequently, two objects which are equivalent under a group transformation, while having the same differential invariants, may have unequal numerical versions, thereby complicating the implementation of their invariant characterization by differential invariant signatures. In our approach, the problem of invariance of the numerical approximation is solved through the introduction of an explicitly group-invariant numerical scheme, based on suitable combinations of joint invariants based on the mesh points used to approximate the object in question. Thus, our schemes are *automatically* invariant under the prescribed transformation group.

Motivations for this approach come from a variety of sources. In modern numerical analysis, the introduction of numerical schemes that incorporate additional structure enjoyed by the problem being approximated have become quite popular in recent years. The first instances of such schemes are the symplectic integrators arising in Hamiltonian mechanics, and the closely allied energy conserving methods; see [14], [33], [54]. Closer in spirit are the invariant numerical schemes for solving partial differential equations studied by Shokin, [50], and Dorodnitsyn, [16].

More specifically, any discrete approximation scheme ultimately relies on introducing a mesh, or discrete number of points, in the submanifold, and then constructing certain appropriate combinations of the coordinates of the mesh points which will approximate the differential invariant quantity of interest. The approximation will be invariant under the underlying transformation group G, and hence its numerical values will not be affected by the group transformations, provided it depends on the various "joint invariants" of the mesh points. In general, if G is any group acting on a space E, then a joint (or algebraic) invariant is a function $J(x^{(1)}, \ldots, x^{(k)})$ depending on several points $x^{(i)} \in E$ having the property that its value is unchanged under *simultaneous* action of the group elements $g \in G$ on the point configuration, so that $J(g \cdot x^{(1)}, \ldots, g \cdot x^{(k)}) = J(x^{(1)}, \ldots, x^{(k)})$. For example, in the case of the Euclidean group, every joint invariant is given as a function of the Euclidean distances $\mathbf{d}(P, Q)$ between pairs of points P, Q, which are the fundamental joint invariants in this case. Similarly, in the case of the equi-affine group, the simplest joint invariant is the area $\mathbf{A}(P, Q, R)$ of the triangle whose vertices are the three points P, Q, R, and, again, every other joint invariant is a function of these triangular area invariants. Results of M. Green [21], generalized in [38], relate the number of differential invariants of curves to the number of joint invariants of the group action, serving as an additional motivation for establishing a more practical connection between the two quantities — a bridge between the discrete and continuous invariant theory.

Consequently, to construct a numerical approximation to a differential invariant I, we employ a finite difference approach, so that the approximation will be computed using appropriate combinations of the coordinates of the mesh points. The approximation will

4

be invariant under the underlying group G, and hence its numerical values will not depend on the group transformations, provided it depends only on the joint invariants of the mesh points. Thus, *any G-invariant numerical approximation to a differential invariant must be governed by a function of the joint invariants of G.* For instance, any Euclidean invariant approximation to the curvature of a plane curve must be based on the distances between the mesh points. The crucial computational issue, then, is to practically determine the appropriate joint invariant which, in the limit as the mesh size goes to zero, recovers the desired differential invariant. In our approach, one interpolates the mesh points with a curve that has a constant value for the differential invariant, using this as the relevant approximation. Practically applicable formulae for Euclidean and affine curvature approximations based on this idea are described below.

An intermediary role is played by the "semi-differential invariants" (or, as we would prefer they be known, "joint differential invariants") introduced into vision by Van Gool *et. al.*, [**34**], [**44**]. Related work appears in the theory of "noise resistant" differential invariants developed by Weiss, [**55**], as well as the local invariant signatures of Bruckstein *et. al.*, [**6**], [**7**], [**8**]. In such an approach, one approximates a higher order differential invariants by a joint differential invariant depending on lower order derivatives evaluated at several points on the curve. In our view, this is only a partial resolution of the difficulty, since to compute any such semi-differential invariant, one must still evaluate each derivative that appears in it by a discrete approximation, and hence the original high order differential invariant is itself approximated in the end by a fully discrete finite difference version. In particular, to maintain invariance of the approximation, one must use a finite difference approximation to the semi-differential invariant by joint invariants, and so one always ends up analyzing the approximation of differential invariants by joint invariants anyway. (On the other hand, one can certainly motivate the construction of useful joint invariant approximations via semi-differential invariants.)

In this paper, we discuss the cases of planar curves under the Euclidean and affine groups in detail, and conclude with an outline of the general theory. A more detailed version of some of these results, including a new approach to the affine geometry of convex curves, appears in the authors' recent paper [**10**].

2. Euclidean Curves in the Plane.

As our first example, we describe the geometry of curves in the Euclidean plane $E \simeq \mathbb{R}^2$. The underlying group is the proper Euclidean group $\mathrm{SE}(2) = \mathrm{SO}(2) \ltimes \mathbb{R}^2$ consisting of rotations, and translations. (One can also readily include reflections, leading to the full Euclidean group $\mathrm{E}(2) = \mathrm{O}(2) \ltimes \mathbb{R}^2$, but the exposition is slightly simpler if we restrict to orientation-preserving Euclidean transformations.) According to Weyl, [**57**], every joint invariant of the Euclidean group is a function of the Euclidean distances $\mathbf{d}(P, Q) = |P - Q|$ between points and the cross-products $(P - Q) \wedge (R - S)$ between displacement vectors. (For the full Euclidean group, only the distances are required since the absolute value of a cross ratio can be expressed in terms of distances.)

Consider a regular, smooth plane curve $\mathcal{C} \subset E$ of class C^2. The simplest differential invariant of the Euclidean group is the Euclidean curvature κ of $\mathcal{C}$, whose value at a point $P \in \mathcal{C}$ is defined as $\pm$ the reciprocal of the radius of the osculating circle to $\mathcal{C}$ at P. The

5

sign is chosen depending on the relative orientation of the circle to the curve — consistent with the condition that convex curves have positive curvature. In terms of a coordinate system such that the part of $\mathcal{C}$ near P is represented by the graph of a function $y = u(x)$, we then have

$$\kappa = \pm \frac{u_{xx}}{(1 + u_x^2)^{3/2}}. \tag{2.1}$$

The Euclidean arc length parameter is defined as $ds = \sqrt{1 + u_x^2}\, dx$, the right hand side representing the simplest invariant one-form for the Euclidean group.

Theorem 2.1. *Every differential invariant of curves in the Euclidean plane is a function of the Euclidean curvature and its derivatives with respect to Euclidean arc length:* $I = F(\kappa, \kappa_s, \kappa_{ss}, \ldots)$.

Remark: The $180°$ rotation $(x, u) \mapsto (-x, -u)$ changes the sign of (2.1), so one cannot do away with the sign ambiguity in the formula. On the other hand, the square κ^2 of the curvature is invariant under the full Euclidean group, including reflections; it and its derivatives with respect to arc length, κ^2, $(\kappa^2)_s$, ..., provide the complete list of Euclidean differential invariants.

Although the successive derivatives of curvature with respect to arc length lead to an infinite hierarchy of higher and higher order differential invariants, as far as the characterization of the curve goes, one only needs to consider the first two: κ and κ_s. This fact motivates the following definition of the signature curve in the Euclidean case, and is formalized in the subsequent theorem, the proof of which follows from the more general results discussed below — see Theorem 5.2.

Definition 2.2. The *Euclidean signature curve* associated with a parametrized plane curve $\mathcal{C} = \{(x(t), y(t))\} \subset E$ is the curve $\mathcal{S} \subset Z \simeq \mathbb{R}^2$ parametrized by the curvature and its first derivative with respect to arc length: $\mathcal{S} = \{(\kappa(t), \kappa_s(t))\} \subset Z$.

Theorem 2.3. *Two smooth (C^3) curves $\mathcal{C}$ and $\overline{\mathcal{C}}$ can be mapped to each other by a proper Euclidean transformation,* $\overline{\mathcal{C}} = g \cdot \mathcal{C}$, $g \in \mathrm{SE}(2)$, *if and only if their signature curves are identical:* $\overline{\mathcal{S}} = \mathcal{S}$.

For example, Figure 4 shows a roughly circular curve, and its Euclidean signature curve, parametrized by (κ, κ_s), immediately below. Note particularly the scale on the signature plot. Indeed, the original curve is described, in polar coordinates, by $r = 3 + \frac{1}{10} \cos \theta$. Its near circularity is reflected by the fact that its signature curve is very small, concentrated near the point $\left(0, \frac{1}{3}\right)$, which is the signature "curve" for a circle of radius 3. The more a curve deviates from circularity, the less concentrated its signature curve becomes — see Figures 6 and 7. Note particularly the increase in complexity and size of the signature curve with the deviation of the original curve from circularity. Angular Fourier modes are characterized by the signature curve's winding around the circular point $\left(0, \frac{1}{3}\right)$.

Euclidean symmetries of a curve are associated with the retracing of the associated signature curve. For example, the three-fold rotational symmetry of the curve in Figure 6 implies that its signature curve is not a simple closed curve, but rather is covered three

times (i.e., has winding number 3) as the original curve is traversed. On the other hand, the curves in Figures 8 and 9 do not admit any Euclidean symmetries and hence their signature curves are only traced once, although they still have winding number 3 with respect to a central point, indicating the existence of an approximate three-fold symmetry. The Euclidean signature curve of the bilaterally symmetric ellipse in Figure 5 is actually traced over twice, owing to the 180° rotational symmetry in the original curve. The reflectional symmetries through the two coordinate axes (which reverse orientation) are manifested by by the reflectional symmetry of the signature curve about the κ axis; this is because the sign of κ has been fixed by the requirement that it be positive for convex curves, whereas κ_s changes sign under such reflections. Alternatively, one could translate this into a retracing by graphing the absolute value of κ_s instead. The most extreme case of retracing occurs for the circles, whose signatures degenerate to a single point, retraced infinitely often; here continual retracing reflects the existence of a one-parameter group of rotational symmetries of the original circle. We conclude that the Euclidean signature curve provides an efficient mechanism for recognizing both exact and approximate Euclidean symmetries of objects.

As a first illustration of our general philosophy of approximating differential invariants by joint invariants, we describe how to use standard geometrical constructions to obtain a numerical approximation to the Euclidean curvature that is unaffected by rigid motions, so that any translated or rotated version of the curve will provide precisely the same numerical approximation for its curvature. We first approximate the parametrized curve by a sequence of mesh points $P_i \in \mathcal{C}$, not necessarily equally spaced. Our goal is to approximate the Euclidean curvature of $\mathcal{C}$ in a Euclidean invariant manner, and, in view of the characterization of Euclidean joint invariants, this requires the approximation to depend only on the distances $\mathbf{d}(P_i, P_j)$ between mesh points. Because the curvature is a second order differential function, the simplest approximation will require three mesh points. With this in mind, we now derive the basic approximation formula for the Euclidean curvature.

Let A, B, C be three successive points on the curve $\mathcal{C}$ such that the Euclidean distances are $a = \mathbf{d}(A, B)$, $b = \mathbf{d}(B, C)$, $c = \mathbf{d}(A, C)$, which are assumed to be small; see Figure 1. The key idea is to use the circle passing through the points A, B, C as our approximation to the osculating circle to the curve at B. Therefore, the reciprocal of its radius $r = r(A, B, C)$ will serve as an approximation to the curvature of the curve at B. Let Δ denote the signed area of the triangle whose vertices are A, B, C, and let $s = \frac{1}{2}(a + b + c)$ denote its semi-perimeter, so that $\Delta = \pm \sqrt{s(s-a)(s-b)(s-c)}$. We apply Heron's formula to compute the radius of the circle passing through the points A, B, C, leading to the exact formula

$$\widetilde{\kappa}(A, B, C) = 4\, \frac{\Delta}{abc} = \pm 4\, \frac{\sqrt{s(s-a)(s-b)(s-c)}}{abc} \tag{2.2}$$

for its curvature. Since formula (2.2) only depends on the Euclidean distances between the three points, it provides us with a completely Euclidean invariant numerical approximation to the curvature of $\mathcal{C}$ at the middle point B. In other words, the approximation for two curves related by a Euclidean motion will be *identical*.

We now need to analyze how closely the numerical approximation $\widetilde{\kappa}(A, B, C)$ is to the true curvature $\kappa(B)$ at the point B. Our analysis is based on a Taylor series expansion — see [10] for a detailed argument.
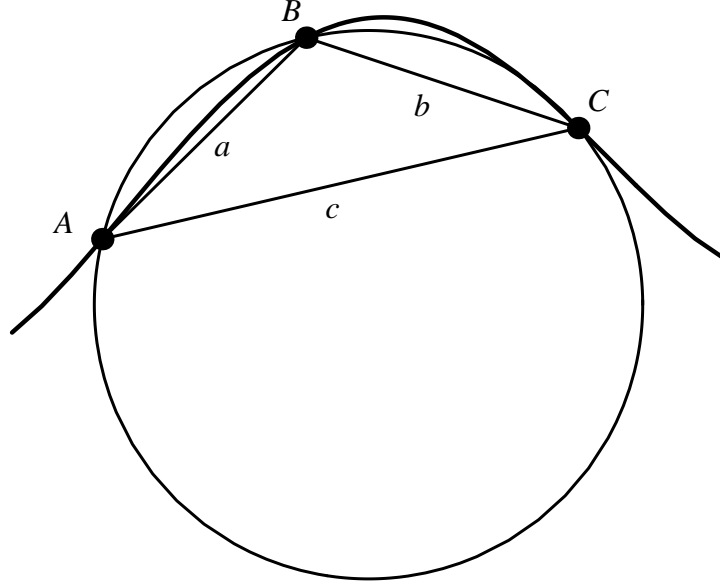
7

Figure 1.   Euclidean Curvature Approximation.

Theorem 2.4. *Let A, B, C be three successive points on the curve $\mathcal{C}$, and let a, b, c be their Euclidean distances. Let $\kappa = \kappa(B)$ denote the Euclidean curvature at B. Let $\widetilde{\kappa} = \widetilde{\kappa}(A, B, C)$ denote the curvature of the circle passing through the three points. Then the following expansion is valid:*

$$\widetilde{\kappa} = \kappa + \frac{1}{3}(b-a)\frac{d\kappa}{ds} + \frac{1}{12}(b^2 - ab + a^2)\frac{d^2\kappa}{ds^2} +$$
$$+ \frac{1}{60}(b^3 - ab^2 + a^2b - a^3)\frac{d^2\kappa}{ds^2} + \frac{1}{120}(b-a)(3b^2 + 5ab + 3a^2)\kappa^2\frac{d\kappa}{ds} + \cdots. \qquad (2.3)$$

In particular, if we choose the points to be equal distance apart, meaning that $a = b$ then the first error term in the approximation (2.3) is of second order. Choosing the three points in the proper order assures us that the sign of the curvature is properly approximated. A proof of the expansion (2.3) appears in the Appendix.

Remark: Since a and b are Euclidean invariants, *every* coefficient of the powers $a^m b^n$ in the series expansion (2.3) must be a Euclidean differential invariant, and hence a function of κ and its arc length derivatives.

The same general method can also be used to find Euclidean-invariant numerical approximations for computing the higher order differential invariants $\kappa_s = d\kappa/ds$, etc. For example, to determine a fully Euclidean invariant finite difference approximation to κ_s, we approximate the Euclidean distance along the curve by the Euclidean distance between the individual mesh points. The elementary finite difference quotient

$$\widetilde{\kappa}_s(P_{i-2}, P_{i-1}, P_i, P_{i+1}) = \frac{\widetilde{\kappa}(P_{i-1}, P_i, P_{i+1}) - \widetilde{\kappa}(P_{i-2}, P_{i-1}, P_i)}{\mathbf{d}(P_i, P_{i-1})}, \qquad (2.4)$$

could be used to approximate $\kappa_s(P_i)$, but suffers from a numerical bias owing to the asymmetry of points chosen to represent the curve near P_i. Therefore, we use the centered difference formula

$$\widetilde{\kappa}_s(P_{i-2}, P_{i-1}, P_i, P_{i+1}, P_{i+2}) = \frac{\widetilde{\kappa}(P_i, P_{i+1}, P_{i+2}) - \widetilde{\kappa}(P_{i-2}, P_{i-1}, P_i)}{\mathbf{d}(P_{i+1}, P_{i-1})}. \qquad (2.5)$$

as the Euclidean invariant approximation to the derivative κ_s. In this manner, we obtain a fully Euclidean invariant discrete approximation to the Euclidean signature curve by using

$$\big(\widetilde{\kappa}(P_{i-1}, P_i, P_{i+1}), \widetilde{\kappa}_s(P_{i-2}, P_{i-1}, P_i, P_{i+1}, P_{i+2})\big) \qquad (2.6)$$

as our approximating points. In the lower two pictures in Figure 4, the original curve has been discretized by choosing 25 points (equally spaced in the angular variable, but not equal Euclidean distance apart). The bottom left figure gives the discrete Euclidean signature curve based on equation (2.4). Note the bias in the vertical direction of the signature points, in contrast with the exact signature curve, which is symmetric about the κ axis. The bottom right picture gives the corresponding unbiased discrete Euclidean signature curve based on the Euclidean invariant approximation (2.6). Further examples of signature curves and their discrete approximations are displayed in Figures 5–9 at the end of the paper. The discrete approximations, based (2.6) with 50 and 100 points in the original curve, are in uniformly excellent agreement with the true signature curve. Of particular note is the non-uniform mesh spacing on the ellipse in Figure 5. The double retracing of the continuous signature curve is more obvious in the discrete versions, where the more widely spaced mesh points produce a slight contraction in the associated discrete signature. The denser discretization provides a much closer approximation, and clearly shows that symmetries in the original curve can still be detected in the signature curve, even when the corresponding discretizations are not uniformly symmetric.

3. Affine Curves in the Plane.

In our second example, we derive a fully affine-invariant finite difference approximation to the affine curvature and arc length of a convex curve in the plane $E \simeq \mathbb{R}^2$. The underlying transformation group is the special affine (or equi-affine) group, denoted $\mathrm{SA}(2) = \mathrm{SL}(2) \ltimes \mathbb{R}^2$ consisting of all area-preserving affine transformations: $\mathbf{x} \to A\mathbf{x} + b$, $\det A = 1$. Thus, the simplest joint affine invariant is the area of a triangle whose vertices are three given points. Given a configuration of points $P_i = (x_i, y_i) \in E$, we define

$$[ijk] = [P_i, P_j, P_k] = (P_i - P_j) \wedge (P_i - P_k) = \det \begin{vmatrix} x_i & y_i & 1 \\ x_j & y_j & 1 \\ x_k & y_k & 1 \end{vmatrix}, \qquad (3.1)$$

so that $[ijk]$ equals the signed area of the parallelogram whose sides are $P_i - P_j$ and $P_i - P_k$, which is twice the signed area of the triangle whose vertices are P_i, P_j, P_k. (The area is positive if the triangle is traversed in a clockwise direction.) According to Weyl, [**57**],
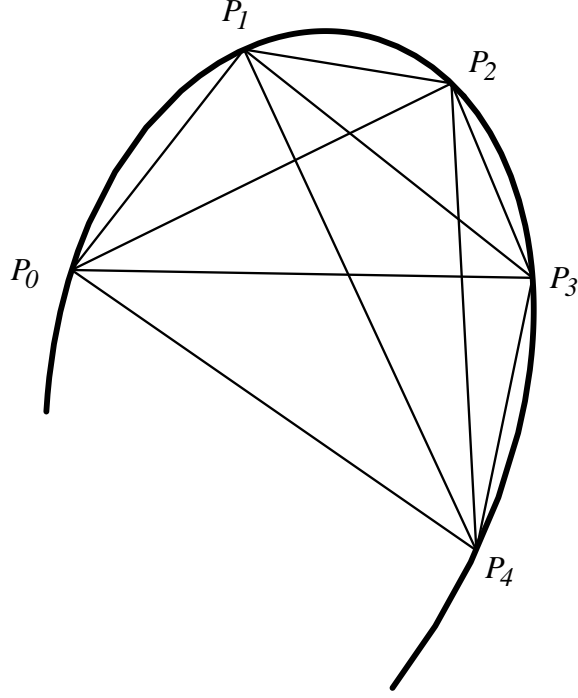
9

Figure 2. The Affine Pentagram.

every joint affine invariant $I(P_1, \ldots, P_n)$ depending on the points P_i is a function of these triangular areas $[ijk]$. A simple example is the useful four-point invariant

$$[ijkl] = [P_i, P_j, P_k, P_l] = (P_i - P_j) \wedge (P_k - P_l) = [ijl] - [ijk], \qquad (3.2)$$

which is a sum of two basic areas (3.1). Like Euclidean distances, the joint affine area invariants are not functionally independent, but are subject to certain relations or "syzygies", which are all consequences of the following:

$$\begin{aligned} [ijl] + [jkl] &= [ijk] + [ikl], \\ [ijk][ilm] - [ijl][ikm] + [ijm][ikl] &= 0. \end{aligned} \qquad (3.3)$$

For example, in a configuration of five points $P_0, \ldots, P_5$, there are 10 possible triangular areas, but only five independent ones; see Figure 2.

Consider a regular, smooth convex[†] plane curve $\mathcal{C} \subset E$ of class C^4. The simplest differential invariant of the equi-affine group is its affine curvature. If we represent the curve as a graph, $y = u(x)$ then the affine curvature is the fourth order differential invariant

$$\kappa = \frac{3u_{xx}u_{xxxx} - 5u_{xxx}^2}{9u_{xx}^{8/3}}. \qquad (3.4)$$

[†] Affine geometry requires the (unfortunate) restriction to convex curves, although many applications to computer vision can dispense with this restriction. For example, the affine-invariant curvature flow can be extended to arbitrary curves by omitting the tangential component; see [47], [40], for details. At the end of this section, we discuss how our approach can be extended to affine-invariant recognition of non-convex curves.

10

Note that κ is undefined at inflection points, where $u_{xx} = 0$, corroborating our restriction to convex curves. The affine arc length element

$$ds = \sqrt[3]{u_{xx}} \; dx \tag{3.5}$$

is the simplest invariant one-form. Thus, the next simplest differential invariant is the derivative

$$\kappa_s = \frac{d\kappa}{ds} = \frac{9u_{xx}^2 u_{xxxxx} - 45u_{xx}u_{xxx}u_{xxxx} + 40u_{xxx}^3}{27u_{xx}^4}. \tag{3.6}$$

of affine curvature with respect to affine arc length.

Theorem 3.1. *Every equi-affine differential invariant for a curve in the plane is a function of the successive derivatives of affine curvature with respect to affine arc length:* $I = F(\kappa, \kappa_s, \kappa_{ss}, \ldots)$.

As with Euclidean curves, the first two differential invariants (3.4), (3.6) suffice to determine a curve uniquely up to an affine transformation.

Definition 3.2. The *affine signature curve* associated with a parametrized convex plane curve $\mathcal{C} = \{(x(t), y(t))\} \subset E$ is the curve $\mathcal{S} \subset Z \simeq \mathbb{R}^2$ parametrized by the affine curvature and its first derivative with respect to affine arc length: $\mathcal{S} = \{(\kappa(t), \kappa_s(t))\} \subset Z$.

Theorem 3.3. *Two smooth* (C^5) *convex curves* $\mathcal{C}$ *and* $\overline{\mathcal{C}}$ *can be mapped to each other by an affine transformation,* $\overline{\mathcal{C}} = g \cdot \mathcal{C}$, $g \in \mathrm{SA}(2)$, *if and only if their signature curves are identical:* $\overline{\mathcal{S}} = \mathcal{S}$.

Theorem 3.3 and Theorem 2.3 are both special cases of Theorem 5.2 below. The Figures at the end of the paper provide a number of illustrations of affine signature curves for convex planar curves. Note particularly the two curves in Figures 8 and 9 are related by the equi-affine transformation $(x, y) \mapsto (x, \frac{1}{2}x + y)$. Their Euclidean signature curves are quite different, whereas their affine signature curves are, of course, identical. As with the Euclidean signatures, affine symmetries of the original curve are indicated by retracing of their affine signature curves.

We now discuss how to construct affine-invariant numerical approximations to affine differential invariants. Note first that, since the affine curvature of a convex curve is a fourth order differential invariant, two smooth, convex curves passing through a common point P have the same equi-affine curvature at P if and only if they have fourth order contact at P. In particular, the affine curvature of a curve $\mathcal{C}$ at P equals the (constant) affine curvature of its *osculating conic* to $\mathcal{C}$ at P, which, by definition, is the unique conic section having fourth order contact to $\mathcal{C}$ at P. We thus need to determine the formula for the affine curvature of a conic section.

Theorem 3.4. *The affine curvature of a nondegenerate conic* $\mathcal{C}$ *defined by the quadratic equation*

$$Ax^2 + 2Bxy + Cy^2 + 2Dx + 2Ey + F = 0 \tag{3.7}$$

is given by

$$\kappa = \frac{S}{T^{2/3}}, \tag{3.8}$$

11

where

$$S = AC - B^2 = \det \begin{vmatrix} A & B \\ B & C \end{vmatrix}, \qquad T = \det \begin{vmatrix} A & B & D \\ B & C & E \\ D & E & F \end{vmatrix}. \qquad (3.9)$$

Remark: Both S and T are equi-affine invariants of the conic. The invariant S vanishes if and only if the five points lie on a parabola. The invariant T vanishes if and only if the conic degenerates to a pair of lines, and hence fails our convexity hypothesis.

In particular, the equi-affine curvature of an ellipse in the plane is given by

$$\kappa = \left(\frac{\pi}{\mathbf{A}} \right)^{2/3}, \qquad \text{where} \qquad \mathbf{A} = \frac{\pi}{\kappa^{3/2}} = -\pi \frac{T}{S^{3/2}} \qquad (3.10)$$

is the area of the ellipse.

As with the osculating circle in the Euclidean case, we now approximate the osculating conic by an interpolating conic passing through five nearby points, and thereby approximate the affine curvature at a point of a plane curve by the affine curvature of the interpolating conic. We will explicitly show how this may be used to produce an affine-invariant finite difference approximation to the affine curvature.

First, we note that five points in general position in the plane determine a unique conic section that passes through them. The explicit formula for the interpolating conic is not difficult to establish; see [**51**] for a proof of the following classical result.

Theorem 3.5. *Let $P_0, \ldots, P_4$ be five points in general position in the plane. There is then a unique conic section $\mathcal{C}$ passing through them, whose quadratic equation has the affine-invariant form*

$$[013][024][\mathbf{x}12][\mathbf{x}34] = [012][034][\mathbf{x}13][\mathbf{x}24], \qquad (3.11)$$

where $\mathbf{x} = (x, y)$ is an arbitrary point on $\mathcal{C}$.

Combining Theorems 3.4 and 3.5, we deduce an explicit formula for the affine curvature of the conic passing through five given points. According to the general result characterizing joint affine invariants, the resulting formula can be written in terms of the 10 triangular areas determined by the points taken three at a time; see Figure 2. Substituting the formulas for the coefficients, we find a particularly nice affine-invariant expression for our first affine invariant

$$4T = \prod_{0 \leq i < j < k \leq 4} [ijk]; \qquad (3.12)$$

in other words, to compute $4T$, multiply together all 10 triangular areas in the pentagram described by the 5 points. The fact that T has such a form is not so surprising, since T vanishes if and only if the conic degenerates to a pair of lines, which requires that three of the five points lie on a line, and hence $[ijk] = 0$ for some $i < j < k$. The simplest

12

affine-invariant formula[†] for S that we know is

$$4S = [013]^2[024]^2[1234]^2 + [012]^2[034]^2[1324]^2 -$$
$$- 2[012][034][013][024]\big([123][234] + [124][134]\big),$$

(3.13)

cf. (3.2). Formula (3.13) is not nearly as pleasant as (3.12), particularly because the right hand side appears to be asymmetrical with respect to permutations of the five points, whereas S must clearly be symmetrical with respect to such permutations. Of course, the explanation lies in the syzygies (3.3) among the triangular areas, a judicious application of which suffices to demonstrate that (3.13) is symmetrical under permutation. A completely symmetrical formula for S can, of course, be obtained by symmetrizing (3.13), i.e., summing over all possible permutations of the set $\{0, 1, 2, 3, 4\}$ and dividing by $5! = 120$, although the result is much more complicated than (3.13). We have been unable to find a simple yet symmetrical version of the formula for S.

As in the Euclidean case, we are interested in finite difference numerical approximations to the affine curvature of a strongly convex plane curve $\mathcal{C}$ which are invariant under the special affine group. We thus approximate the parametrized curve $\mathbf{x}(t)$ by a sequence of mesh points $P_i = \mathbf{x}(t_i)$. Any affine-invariant numerical approximation to the affine curvature κ (as well as any other affine differential invariant $d^n\kappa/ds^n$) must be a function of the joint affine invariants of the mesh points, which means that it must be a function of the areas $[ijk]$ of the parallelograms (or triangles) described by the mesh points. Because the affine curvature is a fourth order differential function, the simplest approximation will require five mesh points, so that the approximation will depend on the ten triangular areas (or, more basically, the five independent areas) in the pentagram whose vertices are the five mesh points, as illustrated in Figure 2.

With this in mind, consider the five successive mesh points $P_{i-2}, P_{i-1}, P_i, P_{i+1}, P_{i+2}$ on the convex curve $\mathcal{C}$. By convexity, the mesh points are in general position, and we let $\mathcal{C}_i = \mathcal{C}(P_{i-2}, P_{i-1}, P_i, P_{i+1}, P_{i+2})$ be the unique conic passing through them. Let $\widetilde{\kappa}_i = \widetilde{\kappa}(P_{i-2}, P_{i-1}, P_i, P_{i+1}, P_{i+2})$ denote the affine curvature of the conic $\mathcal{C}_i$, which we evaluate via the previously established formula

$$\widetilde{\kappa}_i = \frac{S_i}{T_i^{2/3}},$$

(3.14)

where the invariants S_i, T_i are computed in terms of the triangular areas according to equations (3.13) and (3.12), where we replace $P_0, \ldots, P_4$ by $P_{i-2}, \ldots, P_{i+2}$. We now need to analyze how closely the numerical approximation $\widetilde{\kappa}_i$ is to the true curvature $\kappa_i = \kappa(P_i)$ at the middle point P_i. Assuming the points are close together, an extensive MATHEMATICA computation produces the desired Taylor series expansion; the Appendix indicates how this is accomplished.

[†]   Both formula (3.12) and (3.13) were established by direct computation with the aid of MATHEMATICA. The computation is not entirely straightforward, since the intermediate expressions are very long, and are not initially given in terms of the brackets $[ijk]$. Moreover, their reformulation in brackets is not unique, owing to the bracket syzygies (3.3), and thus one must use some ingenuity to arrive at a reasonably simple bracket expression. As far as we know, formulae (3.12) and (3.13) have not appeared in the literature.

13

Theorem 3.6. *Let $P_{i-2}, P_{i-1}, P_i, P_{i+1}, P_{i+2}$ be five successive points on the convex curve $\mathcal{C}$. Let κ be the affine curvature of $\mathcal{C}$ at P_i, and let $\widetilde{\kappa} = \widetilde{\kappa}(P_{i-2}, P_{i-1}, P_i, P_{i+1}, P_{i+2})$ be the affine curvature of the interpolating conic section $\mathcal{C}_i = \mathcal{C}(P_{i-2}, P_{i-1}, P_i, P_{i+1}, P_{i+2})$ passing through the five points. Let*

$$L_j = \mathbf{L}(P_i, P_j; P_{i-2}, P_{i-1}, P_i, P_{i+1}, P_{i+2}) = \int_{P_j}^{P_i} ds, \qquad j = i-2, \ldots, i+2, \qquad (3.15)$$

denote the signed affine arc length of the conic from P_i to P_j; in particular $L_i = 0$. Assuming that each L_j is small, then the following series expansion is valid:

$$\widetilde{\kappa} = \kappa + \frac{1}{5}\left(\sum_{j=i-2}^{i+2} L_j\right)\frac{d\kappa}{ds} + \frac{1}{30}\left(\sum_{i-2 \leq j \leq k \leq i+2} L_j L_k\right)\frac{d^2\kappa}{ds^2} + \cdots. \qquad (3.16)$$

The higher order terms are cubic in the distances L_j.

Remark: The property of "being close" is therefore expressed in an affine-invariant manner as the statement that all the affine arc lengths L_j between mesh points are small. In this way, we are able to introduce a fully affine-invariant notion of "distance," albeit one that requires knowledge of five, rather than two, mesh points.

As in the Euclidean case, we can similarly determine affine-invariant numerical approximations for computing the higher order differential invariants given by the successive derivatives of affine curvature with respect to affine arc length. The starting point is an affine-invariant approximation to the affine arc length measured along the given curve $\mathcal{C}$ between the two mesh points. The obvious candidate for this is to measure distance along the interpolating conic section passing through five successive mesh points. Thus we require an explicit formula for the affine arc length along a conic section. If the conic is an ellipse, then there is a remarkable generalization of the classical formula $\mathbf{A} = \frac{1}{2}rL$, or $L = 2\kappa\mathbf{A}$ relating the area $\mathbf{A}$ of a circular sector to the (Euclidean) arc length L of the circular part of the boundary.

Theorem 3.7. *Let $\mathcal{C}$ be an ellipse. Given points $P, Q \in \mathcal{C}$, let $L = L(P, Q) = \int_P^Q ds$ denote the affine arc length of the arc of the ellipse from P to Q. Then*

$$L = 2\kappa\mathbf{A}, \qquad (3.17)$$

where κ is the affine curvature of $\mathcal{C}$ and $\mathbf{A}$ is the area of the elliptical sector obtained by connecting P and Q to the center of the ellipse by straight line segments — see Figure 3.

Proof: Starting with the general conic equation (3.7), we first invoke the equi-affine change of coordinates

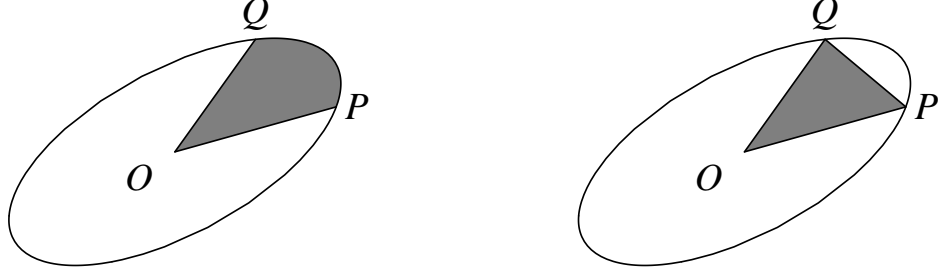$$\tilde{x} = x + \frac{CD - BE}{AC - B^2}, \qquad \tilde{y} = y + \frac{B}{C}x + \frac{E}{C}, \qquad (3.18)$$

14

Figure 3.   Elliptical Sector and its Triangular Approximation.

to place the ellipse in normal form

$$\lambda^2 \tilde{x}^2 + \tilde{y}^2 = \mu^2, \tag{3.19}$$

where, using (3.9),

$$\lambda^2 = \frac{S}{C^2}, \qquad \mu^2 = -\frac{T}{SC}. \tag{3.20}$$

According to (3.8), the affine curvature of either ellipse is given by

$$\kappa = \sqrt[3]{\frac{\lambda^2}{\mu^4}}, \tag{3.21}$$

cf. (3.8). Assume that both $\widetilde{P} = (\tilde{x}_0, \tilde{y}_0)$ and $\widetilde{Q} = (\tilde{x}_1, \tilde{y}_1)$ are on the upper half of the normalized ellipse, so $\tilde{y}_0, \tilde{y}_1 > 0$. (The general case then easily follows.) The affine arc length from $\widetilde{P}$ to $\widetilde{Q}$ can be directly calculated:

$$L(\widetilde{P}, \widetilde{Q}) = \int_{\widetilde{P}}^{\widetilde{Q}} ds = \int_{\tilde{x}_0}^{\tilde{x}_1} \sqrt[3]{\frac{d^2\tilde{y}}{d\tilde{x}^2}} \, d\tilde{x} = -\frac{\mu^{2/3}}{\lambda^{1/3}} \arcsin \frac{\lambda}{\mu} \tilde{x} \Bigg|_{x=\tilde{x}_0}^{\tilde{x}_1}. \tag{3.22}$$

On the other hand, the scaling (non-equi-affine) transformation $(\tilde{x}, \tilde{y}) \mapsto (\tilde{x}, \tilde{y}/\lambda)$ maps the original elliptical sector bounded by $\widetilde{P}$ and $\widetilde{Q}$ to a circular sector bounded by the two points $\widehat{P} = (\tilde{x}_0, \lambda^{-1}\tilde{y}_0)$, $\widehat{Q} = (\tilde{x}_1, \lambda^{-1}\tilde{y}_1)$ lying on a circle of radius $r = \mu/\lambda$. Moreover, the *arcsin* difference term on the right hand side of (3.22) equals $2(\mu^2/\lambda^2)\widehat{\mathbf{A}}$, where $\widehat{\mathbf{A}}$ denotes the area of the circular sector, which is related to the area $\mathbf{A}$ of the elliptical sector according to $\mathbf{A} = \lambda\widehat{\mathbf{A}}$. Therefore,

$$L(\widetilde{P}, \widetilde{Q}) = 2 \frac{\lambda^{5/3}}{\mu^{4/3}} \widehat{\mathbf{A}} = 2 \frac{\lambda^{2/3}}{\mu^{4/3}} \mathbf{A} = 2\kappa\mathbf{A},$$

proving the theorem.   *Q.E.D.*

15

In particular, using equations (3.8), (3.10), we see that the *total* affine arc length **L** of an ellipse equals a multiple of the cube root of its *total* area **A**,

$$\mathbf{L} = 2\kappa\mathbf{A} = \sqrt[3]{8\pi^2 \mathbf{A}} = \frac{2\pi}{\sqrt{\kappa}} = -2\pi \frac{T^{1/3}}{S^{1/2}}, \qquad (3.23)$$

a fact that follows immediately from the classical equi-affine isoperimetric inequality, cf. [**5**]. The explicit formula for the affine arc length along a general conic defined by the quadratic equation (3.7) can be readily deduced from this proof. In the elliptical case, the affine arc length from $P = (x_0, y_0)$ to $Q = (x_1, y_1)$ is given by

$$\int_P^Q ds = \frac{T^{1/3}}{S^{1/2}} \arcsin \sqrt{\frac{-CT}{S^2}} \left(x + \frac{CD - BE}{S} \right) \Bigg|_{x=x_0}^{x_1}. \qquad (3.24)$$

A similar formula can be established in the hyperbolic case.

Remark: It is a curious fact that, in equi-affine geometry, the arc length of an ellipse is given by elementary functions, while in Euclidean geometry, it must be computed via an elliptic integral!

In order to approximate the affine arc length along an arbitrary curve, we use the formula (3.11) to determine the interpolating conic section, and then (3.24) to compute the approximation to the arc length between two successive mesh points. Although the resulting formula is affine invariant by construction, (which is not so obvious from the explicit formula (3.24)), it is not so easy to re-express it directly in terms of the triangular areas (3.1). Indeed, we strongly suspect that the actual formula (guaranteed by the general theory) is a highly complicated transcendental function, and not amenable to explicit computation in this form, although of course, one can readily use (3.24) in conjunction with (3.11) to directly compute the approximate affine arc length in an affine-invariant manner.

An alternative approach is, in the elliptical case, to replace the area of the elliptical sector indicated in Theorem 3.7 by the area of an approximating triangle[†] whose vertices are the two mesh points and the center of the interpolating ellipse — see Figure 3. This does have an explicit formula in terms of the ten triangular areas of the affine pentagram. A direct computation, again with the aid of MATHEMATICA, using (3.11) to compute the quadratic coefficients in (3.7) and (3.18) to determine the coordinates of the center of the ellipse, produces the following formula.

Theorem 3.8. *Let $P_0, \ldots, P_4$ be five points lying on an ellipse. Let O denote the center of the ellipse. Then the area of the triangle with vertices O, P_1, P_3 is given by the affine-invariant formula*

$$\widetilde{\mathbf{A}}(P_1, P_3) = \tfrac{1}{2}[O, P_1, P_3] = \frac{N}{2S}, \qquad (3.25)$$

[†]   Indeed, we are employing a similar device in the Euclidean case, since we should be approximating the Euclidean arc length of the curve by the arc length along the interpolating circle, but, at least to the order of approximation of interest, this can be more simply computed by just using the Euclidean distance between the two mesh points.

where S is given by (3.13), and

$$4N = -[123][134]\left\{[023]^2[014]^2[1234] + [012]^2[034]^2[2314] + \right.$$
$$\left. + [012][023][014][034]([134]-[123])\right\}.$$
(3.26)

Note the remarkable similarity between (3.13) and (3.26)! Equation (3.26) is not fully symmetrical with respect to arbitrary permutations of the five points, but is symmetrical under permutations of P_0, P_2, P_4 and anti-symmetric under interchange of P_1 and P_3. The latter is evident, whereas the former requires use of the syzygies (3.3).

Thus, we obtain an affine-invariant approximation to the arc length along a curve based on a sequence of mesh points by first approximating the curve by an interpolating conic based on five consecutive points; the arc length along the conic is then given by (3.17), and we approximate the elliptical area by the associated triangular area given explicitly in (3.25). The resulting affine arc length approximation can then be used to establish fully affine-invariant approximations to higher order affine differential invariants obtained by differentiating the affine curvature with respect to the affine arc length.

For example, to determine a fully equi-affine invariant finite difference approximation to the derivative κ_s of affine curvature with respect to affine arc length at a mesh point P_i, we use the seven point centered finite difference quotient

$$\widetilde{\kappa}_{s,i} = \frac{\widetilde{\kappa}_{i+1} - \widetilde{\kappa}_{i-1}}{L_i}.$$
(3.27)

Here $\widetilde{\kappa}_i = \widetilde{\kappa}(P_{i-2}, P_{i-1}, P_i, P_{i+1}, P_{i+2})$ denotes the affine curvature of the conic passing through the points $P_{i-2}, P_{i-1}, P_i, P_{i+1}, P_{i+2}$, as given by (3.14). The denominator L_i is the triangular area approximation[†] (3.25) to the affine arc length

$$\mathbf{L}(P_{i-1}, P_{i+1}; P_{i-2}, P_{i-1}, P_i, P_{i+1}, P_{i+2}) = \int_{P_{i-1}}^{P_{i+1}} ds$$
(3.28)

from P_{i-1} to P_{i+1} measured along the same conic, cf. (3.24), and hence is given by

$$L_i = \frac{\widetilde{\kappa}_i N_i}{S_i} = \frac{N_i}{T_i^{2/3}},$$
(3.29)

where S_i and T_i are given by (3.13), (3.12), and N_i by (3.26), where we replace the points P_0, P_1, P_2, P_3, P_4 by $P_{i-2}, P_{i-1}, P_i, P_{i+1}, P_{i+2}$ respectively. Again, we can use these formulae to provide a fully equi-affine invariant numerical approximation to the equi-affine signature curve associated with an arbitrary curve in the plane, and thus perform a fully equi-affine invariant object recognition.

[†] Numerical experiments confirm that the replacement of the more complicated exact formula (3.24) by its triangular approximation makes no significant difference in the accuracy of the approximation, reconfirming that the difference between the two is a higher order term in the error formula.

Remark: The affine arc length of the curve between succesive mesh points P_{i-1} and P_i can be similarly approximated in a fully affine-invariant manner. Summing over all mesh points thereby produces an affine-invariant approximation to the affine arc length of the complete curve.

Some illustrative figures appear at the end of the paper. Note that for the ellipse in Figure 5, the Euclidean signature is not a point, whereas its affine signature curve degenerates to a single point, as does its numerical approximation. Again, the discrete approximations, are in uniformly excellent agreement with the true equi-affine signature curves. The figures were computed in MATHEMATICA; one noticeable effect is the relative speed of computation — the discrete signatures are much faster to compute than the direct continuous version, based on exact symbolic differentiation and substitution to compute the differential invariants. This clearly indicates that, even for regular curves, the numerical implementation offers significant advantages.

Finally, we note on how one might extend the affine signature curve and its discrete approximation to non-convex planar curves. Formulae (3.4), (3.6), reconfirm the fact that the affine curvature κ and its arc-length derivative κ_s are well-defined along any section of the curve that does not contain an inflection point, but both blow up as we approach an inflection point. To understand the behavior, suppose the smooth curve $u = f(x)$ has an inflection point at the origin $x = u = 0$. Substituting the Taylor expansion $u = ax^m + bx^{m+1} + \cdots$, where $m \geq 3$, $a \neq 0$, into (3.4), (3.6), we find that

$$
\begin{aligned}
\kappa &= -\frac{(m-2)(2m-1)}{9m^{2/3}(m-1)^{2/3}a^{2/3}}\, x^{-2(m+1)/3} + \cdots, \\
\kappa_s &= \frac{(m-2)(2m-1)(2m+2)}{27m(m-1)a}\, x^{-(m+1)} + \cdots,
\end{aligned}
\tag{3.30}
$$

give the leading order asymptotics of the signature invariants. Thus as we approach the inflection point, $x \to 0$ and the signature curve tends to ∞ along the asymptotic curve

$$
\kappa_s = \pm C_m |\kappa|^{3/2} + \cdots, \qquad \text{where} \qquad C_m = \frac{2m+2}{\sqrt{(m-2)(2m-1)}}.
\tag{3.31}
$$

Thus, the existence as well as the order of the inflection point is precisely governed by the asymptotics of the associated singularity of the signature curve. For a generic[†] inflection point, $m = 3$, and there is a single asymptotic formula for the blow-up of the signature curve. The detailed behavior of the curve near the inflection point is determined by the higher order terms (in powers of $1/\kappa$) in the asymptotic expansion (3.31).

As for the discrete signature curve, the only way that it can blow up at a mesh point P_i is if the denominator T_i in (3.14) is zero, which means that all five mesh points P_{i-2}, P_{i-1}, P_i, P_{i+1}, P_{i+2}, lie on a straight line. Of course, if this occurs, then there is at least one inflection point lying on that part of the curve lying between P_{i-2} and P_{i+2},

---

[†]   These are the only inflection points surviving a perturbation, and hence the only ones to appear in real images.

and hence the discrete signature has detected an inflection point. (If the T_i vanish over a range of consecutive mesh points, then they all lie on a single straight line, and hence our method will automatically detect straight line components of boundaries of objects.) Barring this unlikely coincidence, the discrete signature curve will continue to consist of computable points, which, as the mesh size gets small, will converge to the continuous affine signature curve on each convex component. Thus, as the mesh size approaches zero, one will detect the asymptotic singularity of the continuous signature curve by a more and more pronounced blow-up of the discrete version; in this manner, the discrete signature curve also distinguishes inflection points in the original curve. The detection of inflection points of non-convex contours in real images is an important ingredient in several proposed object recognition procedures, cf. [46], and their explicit appearance in the signature curve singularity structure, as well as that of its discrete counterpart, lends additional weight to the potential of signature curves to play a significant role in a practical object recognition system.

4. Application to a Medical Image.

The preceding theoretical discussion has demonstrated the feasibility of differential invariant signature curves for recognition of "ideal" boundary curves that could arise in a computer vision image. However, the crucial test of their suitability for genuine applications to object recognition is their robustness in the analysis of real images. Technically speaking, the objects in a real image do not have precisely defined edges, since some amount of blurring or graininess is inherent in the digitalization process. Thus one might be tempted to dismiss the wide variety of object recognition methods based on differential invariants of boundary curves that have been proposed in the literature. Nevertheless, recent successes in invariant segmentation programs based on nonlinear geometric diffusion procedures have shown that, even in very noisy images, one can effectively extract reasonably smooth closed planar curves forming the boundary contours of an objects in the image.

A particularly successful method for edge detection and segmentation in real images has been the method of snakes or active contours, introduced originally by Kass, Witkin and Terzopolous, [26]. (See also the collection of papers in [4].)

A new Euclidean-invariant snake paradigm was recently proposed in [27] and success-fully applied to a wide variety of 2D and 3D medical imagery, including MRI, ultrasound and CT data in [59], [60]. (Similar approaches were independently given in [12] and [49].) A generalization to affine-invariant segmentation was formulated and implemented in [42]. We intend to use these Euclidean or affine-invariant segmentation procedures, in conjunc-tion with the associated nonlinear Euclidean or affine-invariant image smoothing processes, [3], [28], [47], [40], to extract well-defined contours from a noisy image, from which the associated Euclidean or affine signature curve can be computed. In this section, we de-scribe how this procedure has been applied to a particular medical image, demonstrating the robustness of the procedure and its promise for practical invariant object recognition.

Concentrating on the Euclidean case for specificity, the mathematical foundation of the smoothing and segmentation processes is the theory of Euclidean curve shortening,

19

[19], [20], where an initial contour evolves according to the geometric diffusion equation

$$\frac{\partial C}{\partial t} = \kappa \mathbf{N}. \tag{4.1}$$

Here $\mathbf{N}$ is the inward Euclidean unit normal to the curve $C(\cdot, t)$, and κ is the Euclidean curvature. Under this flow, an initially non-convex curve evolves by smoothing into a convex curve, and then becomes asymptotically circular as it shrinks to a point. The associated level set flow, [43], provides a Euclidean-invariant multi-scale smoothing process that has been applied in a wide variety of practical image processing procedures.

Under the curve shortening flow (4.1), the Euclidean perimeter of the evolving curve shrinks as fast as possible, and hence (4.1) can be interpreted as the gradient descent for the Euclidean length functional $\mathcal{L}(C) = \int_C ds$, cf. [27]. Our new active contour method multiplies the Euclidean arc length element ds by a conformal factor $\phi(x, y)$, and computes the associated gradient flow for the modified functional $\mathcal{L}_\phi(C) = \int_C \phi \, ds$. The conformal factor, which depends on the initial image, represents a "stopping term", that is chosen to be small near potential edges, such as regions of high gradient in the image grey level, or regions of contrasting textures. The resulting flow,

$$\frac{\partial C}{\partial t} = \phi \kappa \mathbf{N} - (\nabla \phi \cdot \mathbf{N})\mathbf{N}, \tag{4.2}$$

can be rigorously justified via the method of viscosity solutions, [27], and has been employed to segment even rather noisy medical images; see [59] and [60].

The starting point for the current application was a 70×70, 8-bit gray-scale image of the cross section of a canine heart, obtained from an MRI scan, shown in Figure 10. We applied the Euclidean snake flow (4.2) to extract an approximation to the Euclidean signature curve associated with the boundary of the left ventricle. In addition, curves were obtained from a sequence of images created from this initial image through a successive application of the Euclidean curve shortening smoothing procedure (4.1). We extracted a corresponding sequence of boundary points P_i from each image. A pixel value threshold was fixed to ensure that the boundary was well-defined; pixels with a value less than the threshold value were considered to be part of the bounded area. The boundary points were then extracted in order of orientation. In our numerical experiment, after the initial boundary was extracted, the curve shortening procedure produced a sequence of 60 images through which the boundary curve evolved from its initial shape to a nearly circular contour. As the boundary was shortened from image to image, the number of boundary points dropped from 139 to 89 by the 60th image.

In the computation of the associated differential invariant signatures, two simple Euclidean invariant measures were then taken to compensate for the discreteness of the input data. The first was a process which replaced each point P_i with a weighted average of neighboring points $\frac{1}{10}\left[P_{i-2} + 2P_{i-1} + 4P_i + 2P_{i+1} + P_{i+2}\right]$. This process was applied twice to the data, and had the effect of smoothing out the "jaggedness" of the boundary. The particular weighting used reflects the idea that points which are farther away should be given less weight than near-by points. In addition, the large weight on the point P_i ensured

that the general shape of the curve was not significantly altered. The second measure was taken in the calculation of the curvature approximation $\tilde{\kappa}(P_i)$. Instead of using three successive points in formula (2.2), the values $A = P_{i-5}$, $B = P_i$ and $C = P_{i+5}$ were used. The final step in the process was the calculation of the derivative approximation $\tilde{\kappa}_s(P_i)$ using the centered difference formula (2.5). The resulting set of points $(\tilde{\kappa}(P_i), \tilde{\kappa}_s(P_i))$ provides the desired approximation to the Euclidean signature curve.

A few of the evolving curves and their corresponding signatures are shown in the figures. In Figure 10, the last two pictures show the discrete set of signature points which were calculated for each point on the original contour, and a smooth approximation to the complete signature curve obtained by spline interpolation. In Figure 11 successively smoothed curves, at 10, 20 and 40 time steps in the entire image sequence, are displayed along with their spline-interpolated signature curves. As the evolving curves approach circularity the signature curves exhibit less variation in curvature and appear to be winding more and more tightly around a single point. At any given time this point is the signature "curve" of a circle of area equal to the area inside the evolving curve. Despite the rather extensive smoothing involved, except for an overall shrinking as the contour approaches circularity, the basic qualitative features of the different signature curves, and particularly their winding behavior, appear to be remarkably robust under the curve shortening flow. As in the mathematical examples given above, the windings indicate approximate Euclidean symmetries of the associated contours. These results lead one to speculate that such features can be rather effectively utilized in a practical Euclidean-invariant multi-scale object recognition procedure. A full testing of our methods, as well as their affine-invariant counterparts, on a variety of real-world images, will be reported on in a subsequent publication.

5. General Symmetry Groups.

In the preceding sections, we have concentrated on developing the basic methods for just two symmetry groups — the Euclidean and affine groups for planar curves, a restrciction motivated by their particular importance in computer vision and image processing. However, the basic method of constructing the signature curve and its invariant numerical approximation can, in fact, be applied to any planar group of transformations, including the projective group, so that the Euclidean and equi-affine groups are merely particular cases of a very general methodology. For simplicity of exposition we restrict our attention to the case of planar curves, although generaliztions to surfaces in volumetric images are also covered by the general mathematical theory.

We are interested in the differential invariant signatures associated with a planar curve under a finite-dimensional symmetry group G, acting transitively on the plane. Let us first recall, cf. [**38**], the basic theorem characterizing its differential invariants.

Theorem 5.1. *Let G be an ordinary[†] r-dimensional transformation group acting on $E \simeq \mathbb{R}^2$. Then G admits a unique (up to functions thereof) differential invariant of lowest*

[†]   The technical definition of "ordinary" is that G acts transitively on an open subset of each jet space J^n for $0 \leq n \leq r - 1$. Almost all transformation groups are ordinary. Indeed, the only "non-ordinary" planar group actions are the elementary similarity group $(x, u) \mapsto (\lambda x + c, \lambda u + d)$ and some minor variants thereof. (The fact that x and u scale in exactly the same way is crucial

order, $\kappa(x, u^{(r-1)})$, *having order exactly* $r - 1$, *called the* G-*invariant curvature, and a unique* (*up to constant multiple*) G-*invariant one-form of lowest order,* $ds = P(x, u^{(n)}) \, dx$, *called the* G-*invariant arc length element, whose order is at most* $n \leq r - 2$. *Moreover, every other differential invariant of* G *is a function* $I = I(\kappa, \kappa_s, \kappa_{ss}, \ldots)$ *of the* G-*invariant curvature and its derivatives with respect to the* G-*invariant arc length.*

Remark: Lie, [**31**], completely classified all possible finite-dimensional transformation groups on the plane, up to change of coordinates, and their associated differential invariants; see [**38**] for details.

We define the G-invariant signature curve associated with the parametrized plane curve $\mathcal{C} = \{(x(t), y(t))\}$ to be the curve $\mathcal{S} = \{(\kappa(t), \kappa_s(t))\}$ parametrized by the G-invariant curvature and its first derivative with respect to the G-invariant arc length. The importance of the signature curve lies in the fact that it uniquely characterizes the original curve up to a group transformation. The general result includes the Euclidean and equi-affine cases, Theorems 2.3 and 3.3, as particular cases.

Theorem 5.2. *Let* G *be an ordinary transformation group acting on* $E \simeq \mathbb{R}^2$. *Two smooth* (C^r) *curves* $\mathcal{C}$ *and* $\overline{\mathcal{C}}$ *are equivalent up to a group transformation,* $\overline{\mathcal{C}} = g \cdot \mathcal{C}$, *if and only if their signature curves are identical:* $\overline{\mathcal{S}} = \mathcal{S}$.

Since we believe the proof of Theorem 5.2 is very intuitive and natural, we include it here for the interested reader.

Proof: First note that since κ has order $r - 1$, κ_s has order $r = \dim G$, and so the signature curve requires the computation of rth order derivatives of the parametrizing functions. Generically, the signature curve is given by specifying κ_s as a function of κ, so that $\kappa_s = H(\kappa)$. Therefore, a curve parametrized by a graph $y = u(x)$ will be a solution to the rth order ordinary differential equation

$$\kappa_s(x, u^{(r)}) = H(\kappa(x, u^{(r-1)})) \tag{5.1}$$

determined by its signature curve. Thus, the curve will be uniquely recovered from the signature curve and the initial conditions

$$u(x_0) = y_0, \qquad u_x(x_0) = y_1, \qquad \ldots \qquad u_{r-1}(x_0) = y_{r-1}. \tag{5.2}$$

The proof of Theorem 5.2 can now be completed by using the uniqueness theorem for ordinary differential equations. Indeed, since κ and κ_s are differential invariants, their values are identical for two curves related by a group transformation. Conversely, if the signature curves are identical, the two curves are solutions to the signature equation (5.1) corresponding to two different sets of initial conditions (5.2). Transitivity of $G^{(r-1)}$ on J^{r-1} implies that it acts transitively on the set of possible initial conditions $(x_0, u_0^{(r-1)})$. Let $g \in G$ map the initial conditions for $\mathcal{C}$ to those of $\overline{\mathcal{C}}$. Uniqueness of solutions to the differential equation (5.1) implies that g maps $\mathcal{C}$ to $\overline{\mathcal{C}}$, completing the proof. *Q.E.D.*

— all other similarity groups $(x, u) \mapsto (\lambda x + c, \lambda^\alpha u + d)$, $\alpha \neq 1$, are ordinary.) Non-ordinary groups can also be analyzed, cf. [**38**], but the results are slightly different.

Remark: A fundamental open question is to characterize those signature curves which correspond to closed curves.

Of particular importance are the curves whose G-invariant curvature is a constant, and hence the associated signature curve degenerates to a single point. Such curves play the same role for general transformation groups that the circles and straight lines play for the Euclidean group, and the conic sections play for the equi-affine group. For example, the projective group in the plane, the curves of constant projective curvature are the so-called "W-curves" which were investigated in detail by Klein and Lie, [**29**], [**58**; §III.8].

Theorem 5.3. *Let G be an ordinary transformation group acting on $\mathbb{R}^2$. A curve $\mathcal{C} \subset M$ has constant G-invariant curvature if and only if it is an orbit of a one-parameter subgroup of G, i.e., $\mathcal{C} = \{\exp(t\mathbf{v})P_0\}$ for some infinitesimal generator $\mathbf{v}$ of the group action.*

Like Theorem 5.2, Theorem 5.3 can be proved via standard symmetry group methods for ordinary differential equations. In higher dimensions, there are corresponding, deeper results due to Cartan, that characterize the submanifolds of a homogeneous space up to group transformations via an associated "signature manifold", which is parametrized by the fundamental differential invariants appearing in the invariant Frenet frame on the submanifold. For example, for surfaces in three-dimensional space, the Euclidean signature manifolds are is a surface in a six-dimensional space parametrized by the mean curvature, the Gaussian curvature, and their derivatives with respect to the Euclidean invariant Frenet frame on the surface. A similar construction can be made for the equi-affine geometry of surfaces. See [**11**], [**23**], [**25**], for precise statements and a variety of geometric examples.

Next we discuss how to generalize our construction of invariant numerical approximations to differential invariant signatures. Let $\kappa(P_1)$ be the G-invariant curvature for the plane curve $\mathcal{C}$ at a given point $P_1 \in \mathcal{C}$. Let r be the dimension of G, and choose $r-1$ nearby points $P_2, \ldots, P_r \in \mathcal{C}$. Since the G-invariant curvature $\kappa(x, u^{(r)})$ depends on r^{th} order derivatives, "generically" there exists a unique constant curvature curve $\mathcal{C}_0(P_1, \ldots, P_r)$ passing through them. We let $\widetilde{\kappa}(P_1, \ldots, P_r)$ denote its curvature, which is, by construction, a joint invariant of the chosen points, and forms a G-invariant finite difference approximation

$$\widetilde{\kappa} = \widetilde{\kappa}(P_1, \ldots, P_r) \approx \kappa(P_1) \tag{5.3}$$

to $\kappa(P_1)$. In fact, we conjecture that the following series expansion holds:

$$\widetilde{\kappa} = \kappa + \frac{1}{r}\left(\sum_{j=1}^{r} L_j\right)\frac{d\kappa}{ds} + \frac{1}{r(r+1)}\left(\sum_{1 \le j \le k \le r} L_j L_k\right)\frac{d^2\kappa}{ds^2} + \cdots, \tag{5.4}$$

where κ, $d\kappa/ds$, etc. are evaluated at P_1, and $L_j = \int_{P_1}^{P_j} ds$ denotes the (small) G-invariant "distance" from the point P_1 to P_j, measured as the G-invariant arc length along the constant curvature curve $\mathcal{C}_0$.

Example 5.4. Consider the translation group $(x, u) \mapsto (x + c, u + d)$. In this case, $\kappa = du/dx$, and the constant curvature curves are the straight lines. Then $\widetilde{\kappa}(P_1, P_2) = (u_2 - u_1)/(x_2 - x_1)$. Therefore, the expansion (5.4) is merely the Taylor series, and so

is valid to general order! (Note that since dx is the translation-invariant arc length, the "length" of a straight line segment is $\int_{P_1}^{P_2} dx = x_2 - x_1$.)

Example 5.5. The series expansion (2.3) for the Euclidean curvature is not quite of the form (5.4), since the small parameters should be measured in terms of the Euclidean arc length along the interpolating circle, and not in terms of the direct straight line distance. Thus, we should replace $a = \mathbf{d}(A, B)$ by the circular chord length $L_a = r\theta_a$, where θ_a is the angle measured from the center of the circle between the points A and B. By the Law of Cosines, if $r = 1/\widetilde{\kappa}$ denotes the radius of the circle, we have $a^2 = 2r^2(1 - \cos\theta)$, leading to the series expansions

$$L_a = a + \frac{1}{24}\widetilde{\kappa}^2 a^3 + \frac{3}{640}\widetilde{\kappa}^4 a^5 + \cdots, \qquad a = L_a - \frac{\widetilde{\kappa}^2}{24}L_a^3 + \frac{\widetilde{\kappa}^4}{1920}L_a^5 + \cdots, \qquad (5.5)$$

connecting the circular and straight line distances. Substituting (5.5) into (2.3) produces the revised series expansion

$$\widetilde{\kappa} = \kappa + \frac{1}{3}(L_b - L_a)\frac{d\kappa}{ds} + \frac{1}{12}(L_b^2 - L_a L_b + L_a^2)\frac{d^2\kappa}{ds^2} +$$
$$+ \frac{L_b^3 - L_a L_b^2 + L_a^2 L_b - L_a^3}{60}\frac{d^2\kappa}{ds^2} + \frac{(L_b - L_a)(2L_b^2 + 5L_a L_b + 2L_a^2)}{180}\kappa^2\frac{d\kappa}{ds} + \cdots,$$
$$(5.6)$$

which is the proper Euclidean version of the general series expansion (5.4).

Thus, the conjectured series expansion (5.4) is valid up to order 2 for the translation group, the Euclidean group, and the special affine group. Direct verification for other planar groups appears to be problematic because the explicit formulas for the finite difference approximation $\widetilde{\kappa}$ are not as easy to come by. Moreover, the Euclidean series (5.6) shows that the natural generalization of (5.4) is not valid to order 3. The proof of the second order expansion (5.4), and the determination of higher order terms, remains an important but difficult open problem.

Approximations to the G-invariant arc length from P_1 to P_2, say, are determined by computing the arc length $\mathbf{L}(P_1, P_2) = \int_{P_1}^{P_2} ds$ from P_1 to P_2 along the constant curvature curve $\mathcal{C}_0(P_1, \ldots, P_r)$ passing through them. Thus, one obtains a G-invariant finite difference approximation to the derivative κ_s at a point P_1 by choosing r nearby points $P_2, \ldots, P_{r+1}$ and using the G-invariant difference quotient

$$\widetilde{\kappa}_s = \frac{\widetilde{\kappa}(P_1, \ldots, P_{r-1}, P_r) - \widetilde{\kappa}(P_1, \ldots, P_{r-1}, P_{r+1})}{\mathbf{L}(P_1, P_2)} \approx \kappa_s(P_1), \qquad (5.7)$$

where $\mathbf{L}(P_1, P_2)$ is computed along one of the two possible constant coefficient curves $\mathcal{C}_0(P_1, \ldots, P_{r-1}, P_r)$ or $\mathcal{C}_0(P_1, \ldots, P_{r-1}, P_{r+1})$, or, more symmetrically, their average. As in the Euclidean and affine cases, a centered difference approach should be more accurate. The details and practical implementation of this construction remain to be fully explored.

Formulae (5.3), (5.7) thus provide a completely G-invariant finite difference approximation to the signature curve $\mathcal{S}$ associated with a curve $\mathcal{C} \subset E$, guaranteeing that two

curves related by a group transformation have *identical* discrete signatures. Thus our approach provides a fully group-invariant method for numerically approximating the differential invariant signature curves of *arbitrary* transformation groups. Extensions to surfaces are straightforward in principle, although the precise numerical implementation remains to be fully explored.

6.   Conclusions and Future Applications.

In this paper, we have proposed a new paradigm for the group invariant recognition of visual objects. For objects whose boundaries are described by plane curves, the group-invariant signature curve, which is parametrized by the group-invariant curvature function and its first derivative with respect to the group-invariant arc length element, provides a complete representation of the equivalence class of objects under group transformations, with two curves being mapped into each other if and only if they have identical signature curves. Our experiments with a real medical image strongly indicate that the procedure is not solely of theoretical interest, but has the potential to be practically applied to real image recognition. Therefore, these differential invariant signature curves hold a considerable promise for resolution of a number of key processes in low-level visual recognition systems. The following points indicate some potential (perhaps speculative) applications and extensions.

1. *Recognition and symmetry*: Shape invariants are essential in object recognition since they are independent of the viewpoint in which the given object is observed. Thus an important feature of visual recognition of complex objects is the ability of the detector to find symmetries of objects, or between two similar objects. In the traditional approach, [**24**], [**44**], or the method based invariant indexing functions and frame invariants, [**46**], this requires the identification of distinguished landmark points. Methods that avoid the use of landmarks include the geometric saliency approach of Sato and Cipolla, [**13**], and a method based on matching of moments of Gross and Boult, [**22**]. In the context of signature curves, recognition under group transformations would reduce to the determination of whether the two signature curves (or the appropriate portions thereof) are the same. Similarly, the symmetries of an object are revealed by the fact that the signature curve is retraced, as many times as the number of symmetries. Thus, recognition of objects and symmetries reduces to the problem of determining when parts of two signature curves are identical. In fact, some standard landmark points are automatically represented in the signature curve, e.g., corners produce singularities in both the Euclidean and affine signature curves (with the curve going off to infinity), while inflection points also produce singularities in the affine signature curve.

2. *Tracking*: When objects or cameras move, the continued recognition and tracking of the image is a problem of key importance in vision. The signature curve appears particularly well adapted to this problem, since the signature curve remains unchanged even while the object and or camera is in motion, provided the motions belong to the symmetry group in question, e.g., remain equi-affine. Inclusion of additional transformations, including scaling and projective maps, would cause no additional problem at the theoretical level — one merely uses the corresponding signature curve for the similarity, the full affine, or

even the projective group. See [**15**] for further discussion and applications to the problem of collision avoidance in moving cameras based on image divergence.

3. *Occlusions*: When an object is partially occluded, one can still analyze the unobstructed portion to recognize and reconstruct those parts which lie behind the occlusion. Since the signature curve is purely local, the part of the signature curve corresponding to the unoccluded part remains fixed, and so by comparison with the corresponding portions of known signature curves, one can reasonably expect to continue to recognize and thus reconstruct the object in question. This would be particularly useful in motion and tracking applications, where the temporary occlusion of an object does not affect the signature curve itself, even while the object and or camera is in motion, and thus subject to Euclidean or affine transformations, during the occlusion process.

4. *Real images and noise*: Any method based on the use of differential invariants suffers from the possible high degree of noise caused by the presence of high order derivatives in them. At first glance, the signature curve would appear to compound the problem by incorporating the derivative κ_s into the picture, thereby increasing the order of differentiation by one further degree. Although we still must apply this approach to real image data, there are several avenues that should be cause for optimism. First, segmentation of the curve can be done after some degree of smoothing is performed on the original noisy image. In order to maintain the group invariance, even under denoising, we would advocate a suitably group-invariant geometric diffusion-based smoothing, [**40**], which, in the Euclidean case, means the Euclidean curve shortening flow, [**43**], and, in the affine case, means affine curve shortening, [**47**]. See [**17**], [**39**], [**40**], for generalizations of these flows to other subgroups of the projective group, and [**41**] for further generalizations to arbitrary transformation groups in arbitrary dimensions. Noisy data would produce high rates of change of curvature, and hence spurious outlying portions of the signature curve. One can use various statistical approaches to replace a noisy discrete signature curve by a smooth approximant, including least squares spline fitting, with outlying points either ignored, or having very low weight. An alternative approach would be to smooth the signature curve itself directly before using it to perform recognition of the object. An interesting question is whether a geometric curve shortening flow on the signature curve itself can be constructed in such a manner as to reflect some form of smoothing on the original object.

5. *Discrete invariants*: Every joint invariant based on the discrete mesh points used to approximate a smooth curve provides a discrete invariant signature function. Here, we advocate using those joint invariants that reduce, in the limit as the mesh size goes to 0, to known differential invariants. But any of these discrete invariants could be of use in recognition and tracking problems. The recent preprint of Bruckstein, Rivlin, and Weiss, [**9**], describes related ideas; the crucial (and, in our opinion, tremendously important) distinction is that our approach allows arbitrary discretizations of the curve, whereas in their approach, the distances (or other joint invariant measures) between mesh points is required to be the same, making the actual discretization quite tricky to implement. By allowing arbitrary discretizations, we achieve a far broader range of discrete invariant signatures. The work of Cooper *et. al.*, [**30**], and Rothwell *et. al.*, [**46**], is concerned with a more algebraic use of joint invariants in computer vision; a direct comparison with our approach would be of great interest. Finally, the preprint of Sato and Cipolla,

[**48**], describes an interesting use of integrals of differential invariants and semi-differential invariants in the tracking of curves under motion and occlusion. They use a variant of the signature curve, based on plotting two of these integral invariants, to keep track of the object. The use of such integral invariants provides yet another mechanism for reducing noise in real images.

6. *Comparison of signature curves*: The recognition problem includes a comparison principle that would be able to tell whether two signature curves are close in some sense. Thus, we effectively reduce the group-invariant recognition problem to the problem of imposing a "metric" on the space of shapes, but now by "shape" we mean the signature curve, not the original object. Since the symmetry of an object is manifested by the retracing of its signature curve, one should impose a metric on the space of *weighted curves* An enlightening discussion of possible metrics on shape shape, including Hausdorff, Monge, and variants, appears in [**35**]. Practical issues require that the appropriate metric be noise-resistant; for instance, one might weight outlying parts of the signature curve very low. We are now studying this important issue.

7. *Other symmetry groups*: We have presented explicit formulas for the differential invariant signature curves associated with the Euclidean and equi-affine groups, but the final section indicates how the theory can be readily extended to general continuous transformation groups. The practical implementation, though, requires the introduction of a suitable invariant numerical approximation based on the joint invariants of the group. Even when a classification of these joint invariants is available (e.g., the similarity and projective groups) there is still an important issue that remains as a barrier to the implementation — namely the determination of the formula for the interpolating constant curvature curve through a suitable collection of points. Preliminary computations indicate that, in contrast to the area-preserving cases discussed here, the interpolation equations in general are transcendentally nonlinear and do not admit a readily explicit solution. We are currently at work on means of bypassing this practical complication, with the goal being a suitable group invariant linearization of the interpolation formulae. This will be reported on in a subsequent publication.

8. *Higher dimensional vision*: Although we have concentrated on the use of differential invariants for plane curves, the methods as stated all have higher dimensional analogues, with the key cases being space curves and surfaces. All such variants are handled by Cartan's general theorems, [**11**], which apply to the differential invariants of arbitrary submanifolds under arbitrary transitive transformation groups. For space curves, the corresponding signature curve will be parametrized by the group invariant curvature and torsion, and their derivatives with respect to the group-invariant arc length, and so will be a curve in a four-dimensional signature space. In the case of surfaces under the Euclidean or affine group, there are two fundamental differential invariants (the Gaussian and mean curvatures and their affine analogues, [**23**], [**25**]) that appear in a Frenet frame, and each of them has two invariant derivatives, leading to six fundamental differential invariants in all. Thus, the signature surface will be a two-dimensional submanifold of a six-dimensional signature space. Furthermore, the invariant numerical computation of these differential invariants requires a solution to the interpolation problem, which remains to be investigated.

Appendix. Derivation of Curvature Series Expansions.

In this appendix, we outline how the curvature series expansions (2.3) and (3.16) are derived. Essentially, they are the direct result of a sequence of straightforward, albeit algebraically involved, Taylor series manipulations.

For the Euclidean case, we consider three successive points on the curve A, B, C, as in Figure 1. We can apply a Euclidean transformation so as to arrange $B = (0,0)$, and that the tangent line to the curve to horizontal; for A, C sufficiently close to B we can represent our curve as the graph of a function $y = u(x)$ with $u(0) = 0$, $u_x(0) = 0$, while $A = (h, u(h))$, $C = (k, u(k))$, with $h < 0 < k$ small. We expand in a Taylor series

$$u(h) = \tfrac{1}{2}u_2 h^2 + \tfrac{1}{6}u_3 h^3 + \cdots, \qquad u(h) = \tfrac{1}{2}u_2 h^2 + \tfrac{1}{6}u_3 h^3 + \cdots, \qquad (A.1)$$

where $u_2 = u_{xx}(0)$, $u_3 = u_{xxx}(0)$, etc. (For simplicity we shall just indicate the terms of lowest order, since higher order terms can be readily and systematically generated with sufficient computational stamina (or the aid of a computer algebra system). Since $h < 0 < k$, the two triangular distances have the expansions

$$a = \sqrt{h^2 + u(h)^2} = -h - \tfrac{1}{8}u_2^2 h^3 + \tfrac{1}{12}u_2 u_3 h^4 - \left(\tfrac{1}{48}u_2 u_4 + \tfrac{1}{72}u_3^2\right)h^5 + \cdots,$$
$$b = \sqrt{k^2 + u(k)^2} = k + \tfrac{1}{8}u_2^2 k^3 + \tfrac{1}{12}u_2 u_3 k^4 + \left(\tfrac{1}{48}u_2 u_4 + \tfrac{1}{72}u_3^2\right)k^5 + \cdots.$$

We can invert these series to determine expansions for h and k in terms of the triangular distances:

$$h = -a + \tfrac{1}{8}u_2^2 a^3 + \tfrac{1}{12}u_2 u_3 a^4 + \left(\tfrac{1}{48}u_2 u_4 + \tfrac{1}{72}u_3^2\right)a^5 + \cdots,$$
$$k = b - \tfrac{1}{8}u_2^2 b^3 - \tfrac{1}{12}u_2 u_3 b^4 - \left(\tfrac{1}{48}u_2 u_4 + \tfrac{1}{72}u_3^2\right)b^5 - \cdots.$$

Therefore, the third leg of the triangle can be directly expanded in powers of the other two:

$$
\begin{aligned}
c &= \sqrt{(k-h)^2 + [u(k) - u(h)]^2} \\
&= (k-h)\left[1 + \tfrac{1}{8}u_2^2(h+k)^2 + \tfrac{1}{12}u_2 u_3(h+k)(h^2 + hk + k^2) + \cdots\right] \qquad (A.2)\\
&= (a+b)\left[1 - \tfrac{1}{8}\kappa^2 ab + \tfrac{1}{12}\kappa\kappa_s ab(a-b) - \left\{\tfrac{1}{48}\kappa\kappa_{ss} + \tfrac{1}{128}\kappa^4\right\}ab(a^2 - ab + b^2) + \cdots\right].
\end{aligned}
$$

In the final expression, we utilized the reduced formulae for the values of the curvature and its arc length derivatives at $x = 0$,

$$\kappa(0) = u_2, \qquad \kappa_s(0) = u_3, \qquad \kappa_{ss}(0) = u_4 - 3u_2^3,$$

which are based on our simplification $u_x(0) = 0$. The fact that a, b, c are all Euclidean joint invariants implies that each term in the series (A.2) must be a differential invariant, and hence expressible in terms of κ and its arc length derivatives. Similarly, the area of the triangle in Figure 1 has the expansion

$$
\begin{aligned}
\Delta &= hu(k) - ku(h) \\
&= (h-k)\left[\tfrac{1}{2}u_2 hk + \tfrac{1}{6}u_3 hk(h+k) + \tfrac{1}{24}u_4 hk(h^2 + hk + k^2) + \cdots\right] \qquad (A.3)\\
&= ab(a+b)\left[\tfrac{1}{2}\kappa + \tfrac{1}{6}\kappa_s(b-a) + \tfrac{1}{24}\kappa_{ss}(b^2 - ab + a^2) + \cdots\right].
\end{aligned}
$$

Substituting (A.2), (A.3) (and their higher order terms) into Heron's formula (2.2) completes the proof of (2.3).

The proof of the affine version (3.16) is similar. One uses an affine transformation to place the central point P_i in the affine pentagram at the origin, so that the remaining points have the form $P_{i-2} = (h, u(h))$, $P_{i-1} = (k, u(k))$, $P_{i+1} = (l, u(l))$, $P_{i+2} = (m, u(m))$, for h, k, l, m sufficiently small. The triangular areas are then expanded in Taylor series, as in (A.3), and the result is plugged into the formulae (3.10), (3.13), (3.12), for the affine curvature of the ellipse passing through the mesh points. the resulting Taylor series expansion, after extensive algebraic computation, reduces to (3.16). Owing to the complexity of the calculation, as yet we have not tried to compute any of the higher order terms in the affine expansion.

References

[1] Ackerman, M., and Hermann, R., *Sophus Lie's 1880 Transformation Group Paper*, Math Sci Press, Brookline, Mass., 1975.

[2] Ackerman, M., and Hermann, R., *Sophus Lie's 1884 Differential Invariant Paper*, Math Sci Press, Brookline, Mass., 1976.

[3] Alvarez, L., Lions, P.L., and Morel, J.M., Image selective smoothing and edge detection by nonlinear diffusion, *SIAM J. Numer. Anal.* **29** (1992), 845–866.

[4] Blake, A., and Yuille, A. (editors), *Active Vision*, MIT Press, Cambridge, Mass., 1992.

[5] Blaschke, W., *Vorlesungen über Differentialgeometrie*, Vol. II, J. Springer, Berlin, 1923.

[6] Bruckstein, A.M., Holt, R.J., Netravali, A.N., and Richardson, T.J., Invariant signatures for planar shape recognition under partial occlusion, *CVGIP: Image Understanding* **58** (1993), 49–65.

[7] Bruckstein, A.M., Katzir, N., Lindenbaum, M., and Porat, M., Similarity invariant signatures and partially occluded planar shapes, *Int. J. Comput. Vision* **7** (1992), 271–285.

[8] Bruckstein, A.M., and Netravali, A.N., On differential invariants of planar curves and recognizing partially occluded planar shapes, *Ann. Math. Artific. Int.* **13** (1995), 227–250.

[9] Bruckstein, A.M., Rivlin, E., and Weiss, I., Scale space local invariants, preprint, Technion, Haifa, 1995.

[10] Calabi, E., Olver, P.J., and Tannenbaum, A., Affine geometry, curve flows, and invariant numerical approximations, *Adv. in Math.*, to appear.

[11] Cartan, É., *La Méthode du Repére Mobile, la Théorie des Groupes Continus, et les Espaces Généralisés*, Exposés de Géométrie No. 5, Hermann, Paris, 1935.

[12] Caselles, V., Kimmel, R., and Sapiro, G., Geodesic snakes, *Int. J. Computer Vision*, to appear.

[13] Cham, T.-J., and Cipolla, R., Geometric saliency of curve correspondences and grouping of symmetric contours, preprint, Dept. of Engineering, Univ. of Cambridge, 1995.

[14] Channell, P.J., and Scovel, C., Symplectic integration of Hamiltonian systems, *Nonlinearity* **3** (1990), 231–259.

[15] Cipolla, R., and Blake, A., Image divergence and deformation from closed curves, preprint, Dept. of Engineering, Univ. of Cambridge, 1995.

[16] Dorodnitsyn, V.A., Symmetry of finite difference equations, in: *CRC Handbook of Lie Group Analysis of Differential Equations*, Vol. 1, Ibragimov, N.H., ed., CRC Press, Boca Raton, Fl., 1994, pp. 349–403.

[17] Faugeras, O., On the evolution of simple plane curves of the real projective plane, *Comptes Rendus Acad. Sci. (Paris), Série I*, **317** (1993), 565–570.

[18] Faugeras, O., and Keriven, R., Scale-spaces and affine curvature, in: *Proc. Europe–China Workshop on Geometrical Modelling and Invariants for Computer Vision*, R. Mohr and C. Wu (eds.), 1995, pp. 17–24.

[19] Gage, M., and Hamilton, R.S., The heat equation shrinking convex plane curves, *J. Diff. Geom.* **23** (1986), 69–96.

[20] Grayson, M., The heat equation shrinks embedded plane curves to round points, *J. Diff. Geom.* **26** (1987), 285–314.

[21] Green, M.L., The moving frame, differential invariants and rigidity theorems for curves in homogeneous spaces, *Duke Math. J.* **45** (1978), 735–779.

[22] Gross, A.D., and Boult, T.E., Analyzing skewed symmetries, *Int. J. Comput. Vision* **13** (1994), 91–111.

[23] Guggenheimer, H.W., *Differential Geometry*, McGraw–Hill, New York, 1963.

[24] Huttenlocher, D.P., and Ullman, S., Recognising solid objects by alignment with an image, *Int. J. Computer Vision* **5** (1990), 195–212.

[25] Jensen, G.R., *Higher order contact of submanifolds of homogeneous spaces*, Lecture Notes in Math., No. 610, New York, Springer–Verlag, 1977.

[26] Kass, M., Witkin, A., and Terzopoulos, D., Snakes: active contour models, *Int. J. Computer Vision* (1988), 321–331.

[27] Kichenassamy, S., Kumar, A., Olver, P.J., Tannenbaum, A., and Yezzi, T., Conformal curvature flows: from phase transitions to active vision, *Arch. Rat. Mech. Anal.*, to appear.

[28] Kimia, B., Tannenbaum, A., and Zucker, S., Shapes, shocks and deformations I: The components of two-dimensional shape and reaction-diffusion space, *Int. J. Comp. Vision* **15** (1995), 189–224.

[29] Klein, F., and Lie, S., Über diejenigen ebenen Curven, welche durch ein geschlossenes System von einfach unendlich vielen vertauschbaren linearen Transformationen in sich übergeben, *Math. Ann.* **4** (1871), 50–84.

[30] Lei, Z., Keren, D., and Cooper, D.B., Recognition of complex free-form objects based on mutual algebraic invariants for pairs of patches of data, preprint, Brown University, 1995.

[31] Lie, S., Theorie der Transformationsgruppen I, *Math. Ann.* **16** (1880), 441–528; also *Gesammelte Abhandlungen*, Vol. 6, B.G. Teubner, Leipzig, 1927, pp. 1–94; see [**1**] for an English translation.

[32] Lie, S., Über Differentialinvarianten, *Math. Ann.* **24** (1884), 537–578; also *Gesammelte Abhandlungen*, Vol. 6, B.G. Teubner, Leipzig, 1927, pp. 95–138; see [**2**] for an English translation.

[33] Marsden, J.E., *Lectures on Mechanics*, Cambridge Univ. Press, London, 1992.

[34] Moons, T., Pauwels, E., Van Gool, L., and Oosterlinck, A., Foundations of semi-differential invariants, *Int. J. Comput. Vision* **14** (1995), 25–48.

[35] Mumford, D., Mathematical theories of shape: Do they model perception?, *in*: *Geometrical Methods in Computer Vision*, SPIE Proceedings, Vol. 1570, San Diego, 1991, pp. 2–10.

[36] Mundy, J.L., and Zisserman, A. (eds.), *Geometric Invariance in Computer Vision*, The MIT Press, Cambridge, Mass., 1992.

[37] Mundy, J.L., Zisserman, A., and Forsyth, D. (eds.), *Applications of Invariance in Computer Vision*, Springer–Verlag, New York, 1994.

[38] Olver, P.J., *Equivalence, Invariants, and Symmetry*, Cambridge University Press, 1995.

[39] Olver, P.J., Sapiro, G., and Tannenbaum, A., Classification and uniqueness of invariant geometric flows, *Comptes Rendus Acad. Sci. (Paris), Série I,* **319** (1994), 339–344.

[40] Olver, P.J., Sapiro, G., and Tannenbaum, A., Differential invariant signatures and flows in computer vision: a symmetry group approach, *in*: *Geometry–Driven Diffusion in Computer Vision*, B. M. Ter Haar Romeny, ed., Kluwer Acad. Publ., Dordrecht, the Netherlands, 1994, pp. 205–306.

[41] Olver, P.J., Sapiro, G., and Tannenbaum, A., Invariant geometric evolutions of surfaces and volumetric smoothing, *SIAM J. Appl. Math.*, to appear.

[42] Olver, P.J., Sapiro, G., and Tannenbaum, A., Affine invariant edge maps and active contours, preprint, University of Minnesota, 1995.

[43] Osher, S.J., and Sethian, J.A., Front propagation with curvature dependent speed: Algorithms based on Hamilton–Jacobi formulations, *J. Comp. Phys.* **79** (1988), 12–49.

[44] Pauwels, E., Moons, T., Van Gool, L.J., Kempenaers, P., and Oosterlinck, A., Recognition of planar shapes under affine distortion, *Int. J. Comput. Vision* **14** (1995), 49–65.

[45] ter Haar Romeny, B. (editor), *Geometry–Driven Diffusion in Computer Vision*, Kluwer, Holland, 1994.

[46] Rothwell, C.A., Zisserman, A., Forsyth, D.A., and Mundy, J.L. , Planar object recognition using projective shape representation, *Int. J. Comput. Vision* **16** (1995), 57–99.

[47] Sapiro, G., and Tannenbaum, A., On affine plane curve evolution, *J. Func. Anal.* **119** (1994), 79–120.

[48] Sato, J., and Cipolla, R., Invariant signatures and outlier detection, preprint, Dept. of Engineering, Univ. of Cambridge, 1995.

[49] Shah, J., Recovery of shapes by evolution of zero crossings, preprint, Department of Mathematics, Northeastern University, Boston, 1995.

[50] Shokin, Yu. I., *The Method of Differential Approximation*, Springer–Verlag, New York, 1983.

[51] Sturmfels, B., *Algorithms in Invariant Theory*, Springer–Verlag, New York, 1993.

[52] Van Gool, L., Moons, T., Pauwels, E., and Oosterlinck, A., Semi-differential invariants, in: *Applications of Invariance in Computer Vision*, J.L. Mundy and A. Zisserman, eds., Springer–Verlag, New York, 1994, pp.157–192.

[53] Van Gool, L., Moons, T., Pauwels, E., and Oosterlinck, A., Vision and Lie's approach to invariance, *Image and Vision Comp.* **13** (1995), 259–277.

[54] van Beckum, F.P.H., and van Groesen, E., Discretizations conserving energy and other constants of the motion, in: *Proc. ICIAM 87*, Paris, 1987, pp. 17–35 .

[55] Weiss, I., Geometric invariants and object recognition, *Int. J. Comp. Vision* **10** (1993), 207–231.

[56] Weiss, I., Noise-resistant invariants of curves, *IEEE Trans. Pattern Anal. Machine Intelligence* **15** (1993), 943–948.

[57] Weyl, H., *Classical Groups*, Princeton Univ. Press, Princeton, N.J., 1946.

[58] Wilczynski, E.J., *Projective Differential Geometry of Curves and Ruled Surfaces*, B.G. Teubner, Leipzig, 1906.

[59] Yezzi, A., Kichenassamy, S., Kumar, A., Olver, P.J., and Tannenbaum, A., Geometric snakes for edge detection and segmentation of medical imagery, *IEEE Trans. Medical Imaging*, to appear.

[60] Yezzi, A., Kichenassamy, S., Olver, P., and Tannenbaum, A., A gradient surface approach to 3D segmentation, *Proceedings of IS&T*, to appear.
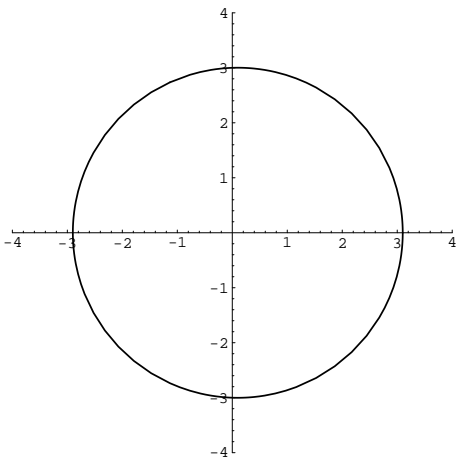
The Original Curve
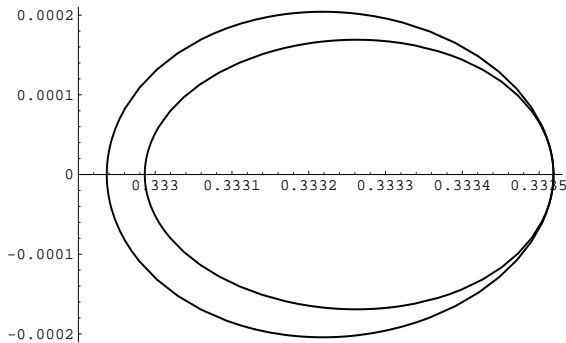
Euclidean Signature Curve
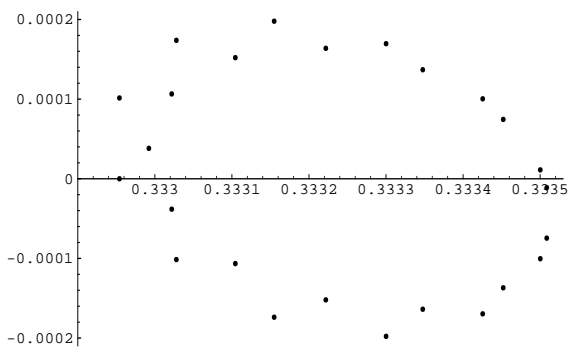
Biased Discrete
Euclidean Signature
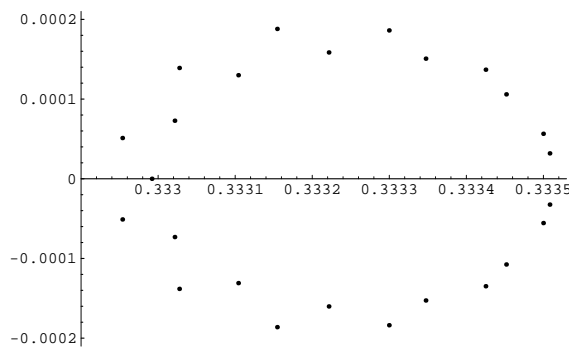
UnBiased Discrete
Euclidean Signature

Figure 4.   The Polar Curve $r = 3 + \frac{1}{10}\cos\theta$.
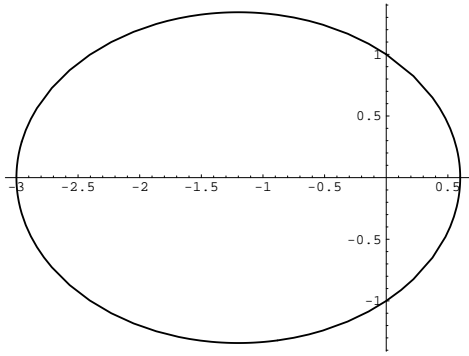
The Original Ellipse
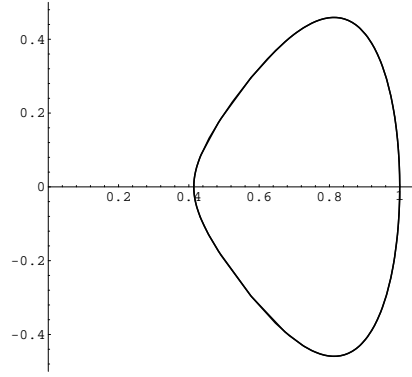
Euclidean Signature Curve
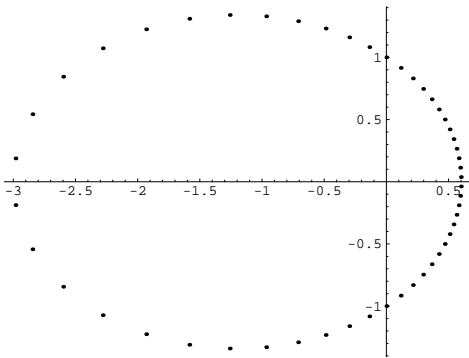
Discretization with 50 Points
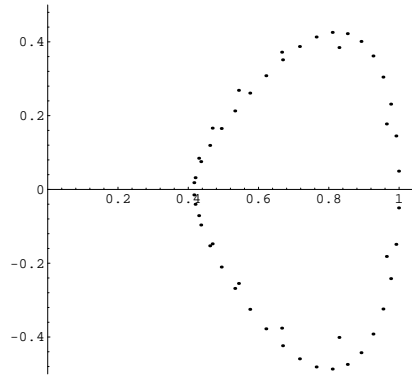
Discrete Euclidean Signature
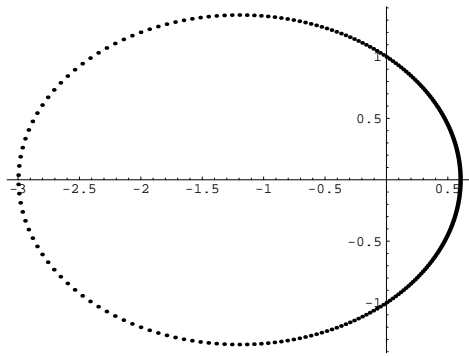
Discretization with 250 Points
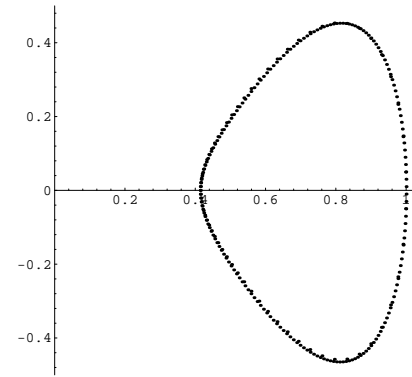
Discrete Euclidean Signature

Figure 5. The Ellipse $r\left(1 + \frac{2}{3}\sin\theta\right) = 1$.
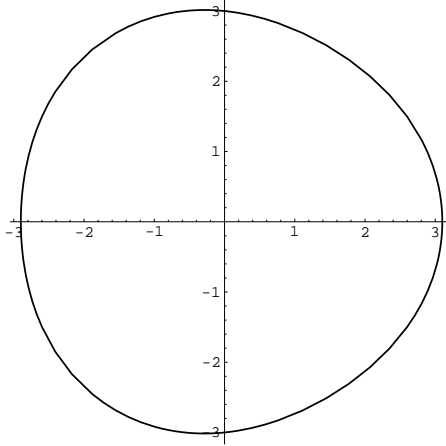
The Original Curve
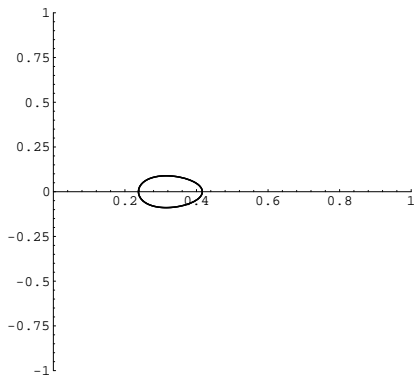
Euclidean Signature Curve
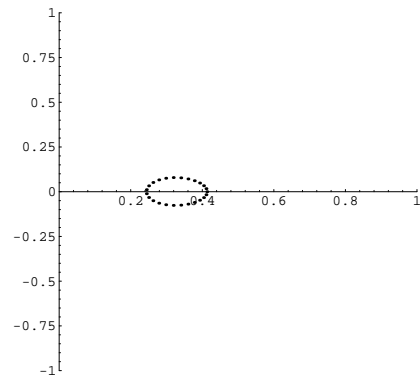
Discrete Euclidean Signature
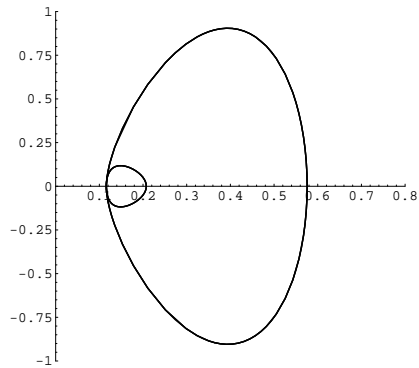
Affine Signature Curve
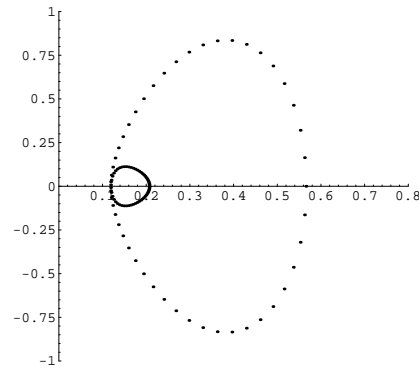
Discrete Affine Signature

Figure 6.   The Polar Curve $r = 3 + \frac{1}{10}\cos 3\theta$.
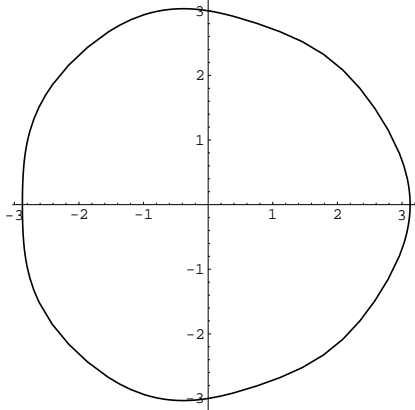
The Original Curve
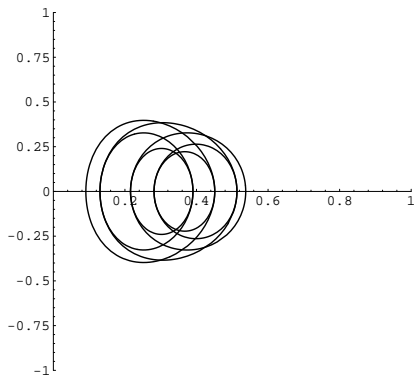
Euclidean Signature Curve
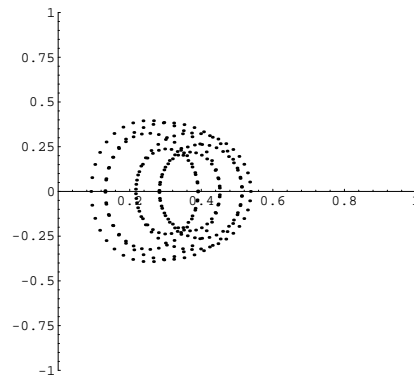
Discrete Euclidean Signature
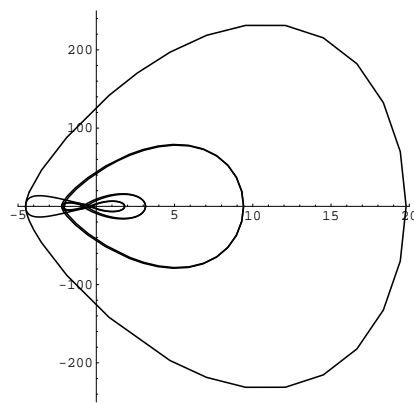
Affine Signature Curve
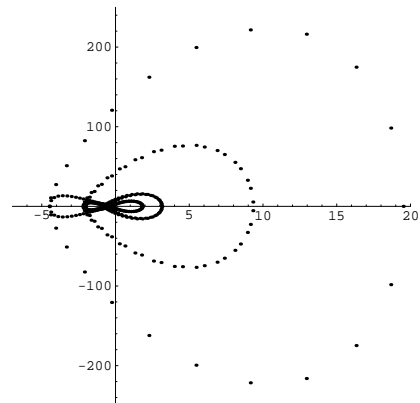
Discrete Affine Signature

Figure 7.   The Polar Curve $r = 3 + \frac{1}{10}\cos 3\theta + \frac{1}{40}\cos 7\theta$.
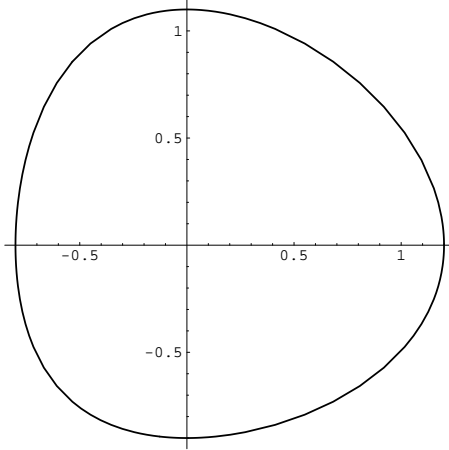
The Original Curve
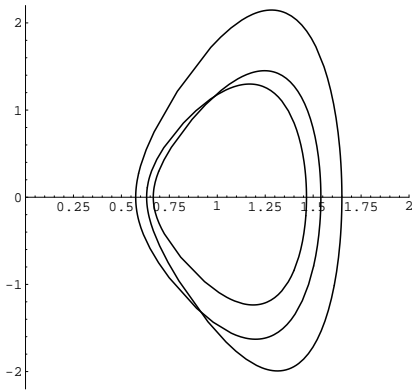
Euclidean Signature Curve
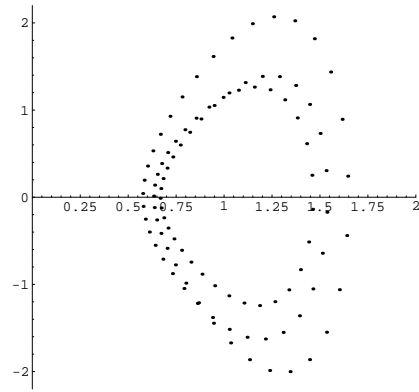
Discrete Euclidean Signature
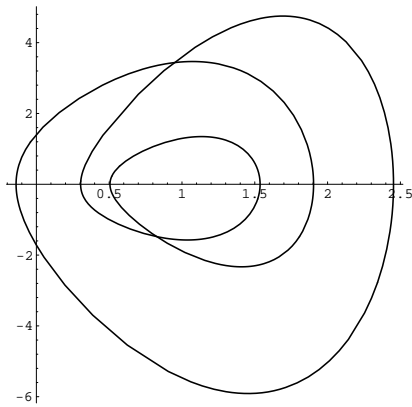
Affine Signature Curve
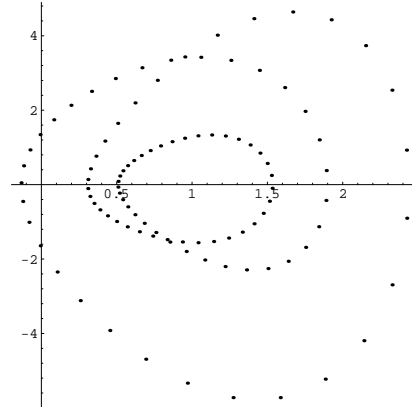
Discrete Affine Signature

Figure 8.   The Curve $x = \cos t + \frac{1}{5}\cos^2 t$, $y = \sin t + \frac{1}{10}\sin^2 t$.
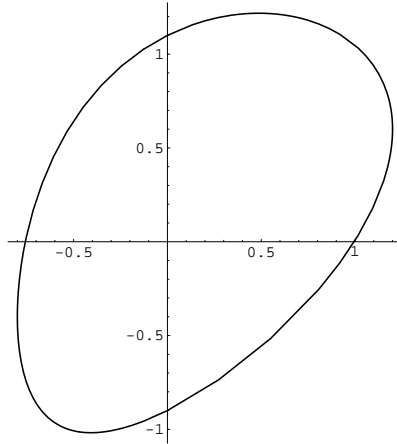
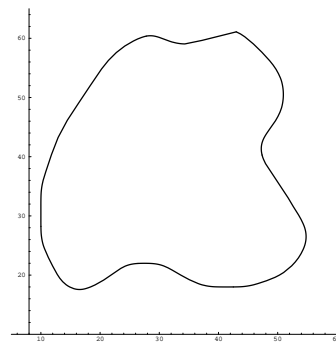The Original Curve
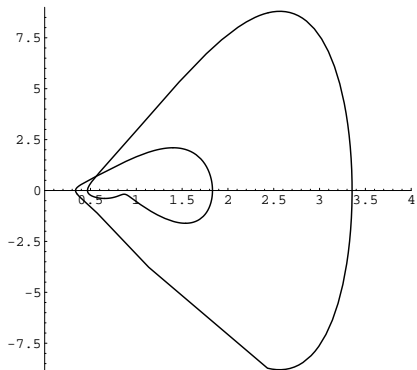
Euclidean Signature Curve
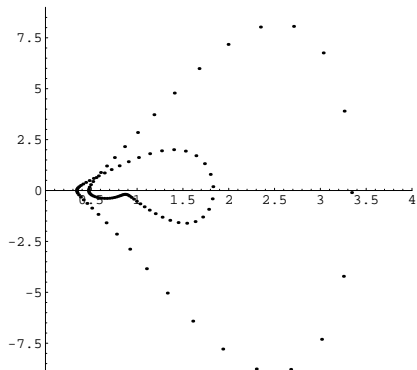
Discrete Euclidean Signature
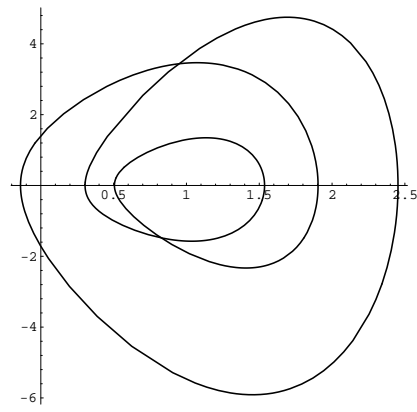
Affine Signature Curve
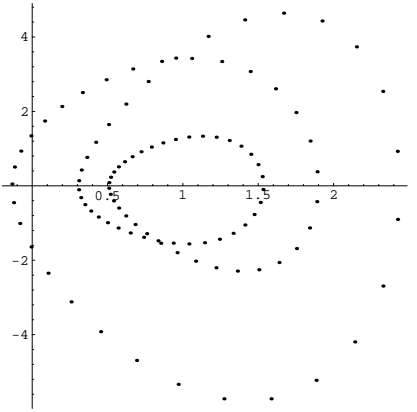
Discrete Affine Signature

Figure 9.   The Curve $x = \cos t + \frac{1}{5} \cos^2 t$, $y = \frac{1}{2}x + \sin t + \frac{1}{10} \sin^2 t$.
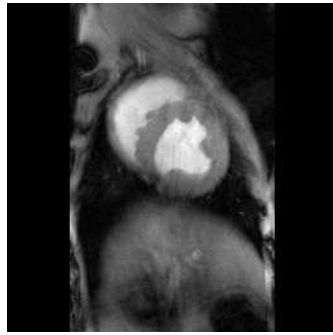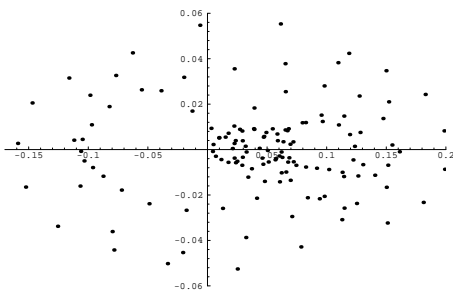
Original Canine Heart
MRI Image
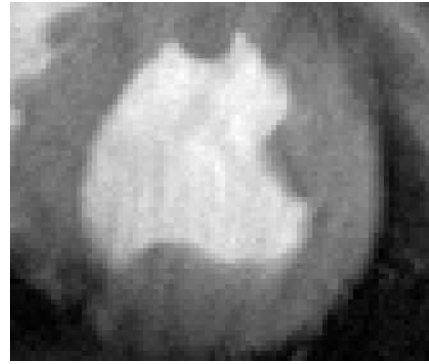
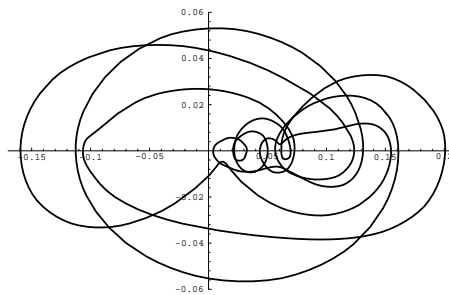Blow Up of the Left Ventricle
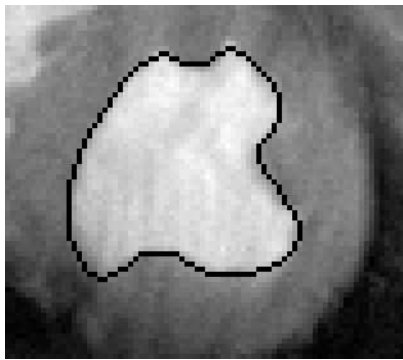
Boundary of Left Ventricle

Original Contour

Discrete Euclidean Signature

Smoothly Connected
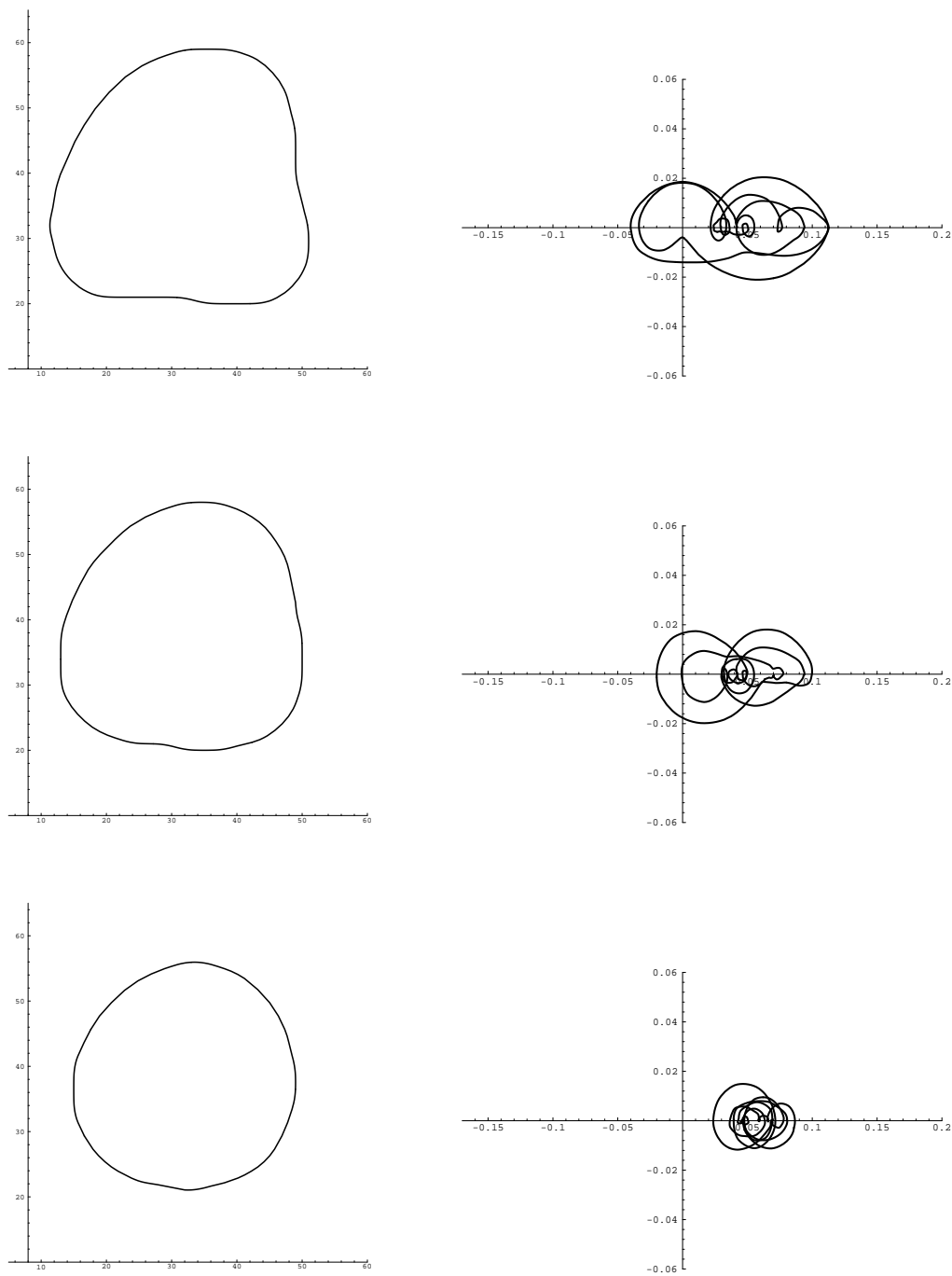Euclidean Signature

Figure 10.   Canine Left Ventricle Signature.

Figure 11.   Smoothed Canine Left Ventricle Signatures.